Research Square

Preprints are preliminary reports that have not undergone peer review.
They should not be considered conclusive, used to inform clinical practice,
or referenced by the media as validated information.

Harris Hawks Optimized Fuzzy-FOPID Control for Pressure–Flow and Torque-Ripple Regulation in a Worn Radial Piston Pump

Neeraj Kumar

neeraj.kumar@sitpune.edu.in

Symbiosis International (Deemed University)

Paladugu Venkaiah

Guru Nanak Institute of Technology

Vineet Kumar

Madanapalle Institute of Technology and Science (MITS), Deemed to be University

Bikash Kumar Sarkar

National Institute of Technology Meghalaya

Research Article

Keywords: Radial piston pump, Piston–cylinder wear, Harris Hawks Optimization, Fuzzy-FOPID control, Pressure–flow regulation, Torque-ripple reduction

Posted Date: November 13th, 2026

DOI: https://doi.org/10.21203/rs.3.rs-11401049/v1

License: This work is licensed under a Creative Commons Attribution 4.0 International License.
Read Full License

Additional Declarations: No competing interests reported.

Harris Hawks Optimized Fuzzy-FOPID Control for Pressure–Flow and Torque-Ripple Regulation in a Worn Radial Piston Pump

[1*]Neeraj Kumar, [2]Paladugu Venkaiah, [3]Vineet Kumar, [4]Bikash Kumar Sarkar

[1]Robotics and Automation, Symbiosis Institute of Technology, Pune Campus, Symbiosis International (Deemed University), Pune, Maharashtra, India-412115

[2]Department of Mechanical Engineering, Guru Nanak Institute of Technology, Hyderabad, India-500100

[3]Department of Electrical and Electronics Engineering, Madanapalle Institute of Technology and Science (MITS), Deemed to be University, Madanapalle, Andhra Pradesh, India – 517325

[4]Department of Mechanical Engineering, National Institute of Technology Meghalaya, India - 793108

Highlights

1. A nonlinear wear-dependent model of a nine-piston radial piston pump has been formulated by considering piston kinematics, internal leakage, manifold compressibility, and shaft-torque dynamics.
2. Progressive piston–cylinder clearance has been shown to produce coupled pressure–flow degradation and a marked increase in shaft-torque ripple.
3. A two-stage HHO-tuned Fuzzy-FOPID strategy has been developed for coordinated hydraulic regulation and mechanical torque-ripple suppression.
4. The proposed controller reduces pressure, flow, and torque RMSE by 79.56%, 80.09%, and 66.49%**,** respectively, under severe wear.
5. Robust regulation has been maintained over the complete wear range without actuator saturation or wear-dependent controller retuning.

Abstract

Radial piston pumps are widely used in high-pressure hydraulic drives, industrial machinery, and precision actuation systems because of their high power density and efficient pressure delivery. However, progressive piston–cylinder wear increases internal leakage, degrades pressure and flow regulation, and introduces undesirable shaft-torque fluctuations. In this work, a nine-piston radial piston pump has been mathematically modeled by considering piston kinematics, pressure-dependent leakage, manifold compressibility, load-flow characteristics, and shaft-torque dynamics. Progressive wear has been represented through an increase in piston–cylinder radial clearance from 16 to 32 μm, and the developed model has been validated against published pump data. A Harris Hawks Optimization tuned Fuzzy Fractional-Order PID controller has then been proposed for coordinated pressure–flow regulation and torque-ripple suppression. The complete nonlinear model, optimization procedure, and controller assessment have been implemented in MATLAB. The open-loop analysis has shown that severe wear increases mean leakage by about 67.4%, while pressure, flow, and shaft-torque ripples rise from 0.73%, 0.37%, and 1.95% to 9.55%, 4.88%, and 10.95%, respectively. Under a 9.29–10.79 MPa step demand and severe wear, the proposed HHO-Fuzzy-FOPID reduces the pressure, flow, and torque RMSE by approximately 79.56%, 80.09%, and 66.49% relative to the uncontrolled case. The controller has also maintained bounded actuator action without saturation and stable performance over the complete wear range. The results demonstrate the effectiveness of the proposed approach for robust hydraulic regulation and torque-ripple mitigation in degraded radial piston pump.

Keywords: *Radial piston pump; Piston–cylinder wear; Harris Hawks Optimization; Fuzzy-FOPID control; Pressure–flow regulation; Torque-ripple reduction*

1. Introduction

Radial piston pumps are positive-displacement hydraulic machines capable of delivering high pressure with compact size, high power density, and good volumetric efficiency. These characteristics have made them attractive for industrial hydraulic power units, mobile machinery, high-pressure test systems, hydrostatic transmissions, and other applications in which a stable pressure-flow supply is required. Recent studies have continued to develop mathematical and experimental models of piston-radial pumps for mobile hydraulic systems and have demonstrated their applicability over a wide range of operating conditions [1]. Radial piston concepts have also been investigated for low-speed hydrostatic transmissions in small hydropower plants, where high efficiency and pulsation attenuation are important design requirements [2]. In conventional high-pressure applications, however, the useful advantages of radial piston pumps can be limited by

periodic flow fluctuation, pressure pulsation, internal leakage, and torque variation. Accordingly, valve-plate configuration, transition-zone geometry, silencing grooves, and pump-control strategies have received considerable attention [3-7].

The dynamic behaviour of a piston pump is strongly influenced by the coupled interaction between piston kinematics, fluid compressibility, leakage paths, chamber pressure, port timing, manifold dynamics, and the external hydraulic load. Bergada et al. [8] developed a detailed analytical treatment of piston-pump leakage and output-flow ripple and showed that clearance flows and pressure dynamics must be considered together when predicting pump behaviour. Xu et al. [9] reported that the flow ripple of a piston pump is affected by several operating and fluid parameters, including leakage, oil viscosity, compressibility, entrained air, and working conditions. The effect of oil compressibility on flow pulsation has also been discussed in [10]. Apart from the hydraulic response, the periodic pressure developed inside the pump can also produce vibration and variation in shaft loading. Ye et al. [11] studied the contribution of pump excitation forces to vibration. Different valve-plate modifications, including triangular and U-shaped damping grooves, have been investigated to reduce flow ripple [12,13], while erosion near the damping holes has also been reported as an important durability issue [14]. Manring and Zhang [15] discussed the influence of trapped volume and valve-plate design on volumetric efficiency, whereas Pan et al. [16] showed that swash-plate motion can affect outlet-flow and pressure pulsations. Most of these studies have been carried out for axial piston pumps; however, the basic effects of fluid compressibility, leakage through clearances, periodic piston delivery, and pressure-induced torque variation are also important for modelling radial piston pump.

Wear of the piston-cylinder pair is particularly important because the operating clearance simultaneously provides lubrication and forms a major internal leakage path. As the clearance increases due to friction, contamination, surface damage, or long-term operation, leakage rises rapidly and the effective delivery of the affected piston decreases. Bensaad et al. [17] showed that a leaky piston disturbs the outlet-pressure signal, reduces pump efficiency, and produces vibration signatures that can be used for fault identification. More recent work has treated the leakage coefficient itself as a health indicator for estimating piston-pump wear severity [18]. Physics-informed approaches have also been proposed for identifying friction-pair wear and estimating internal degradation from pump responses [19], while flow-ripple information has increasingly been used as a fault-sensitive quantity for piston-pump condition monitoring [20]. These studies demonstrate the close relationship between wear, leakage, pressure fluctuation, and mechanical vibration. However, most wear-oriented investigations have concentrated on fault detection,

diagnosis, or performance prediction rather than closed-loop compensation of the hydraulic and mechanical degradation caused by wear.

Pressure regulation of piston pumps has traditionally been addressed using hydro-mechanical compensators, PID control, variable-speed drives, and nonlinear model-based techniques. Kemmetmuller et al. [21] developed nonlinear pressure control for self-supplied variable-displacement piston pumps subjected to fast and unknown load changes. Helian et al. [22] later proposed an adaptive robust pressure controller based on a reduced-order pump model and demonstrated improved tracking under nonlinearities, uncertainty, and time-varying disturbances. For aviation hydraulic systems, Zhang and Li [23] investigated PID, LQR, and backstepping-based approaches for continuously regulated piston-pump pressure. In the radial-piston-pump context, conventional PID-based pressure-control studies have demonstrated the feasibility of regulating delivery pressure through displacement or speed variation [6,7], but classical PID performance is inevitably dependent on fixed gains and may deteriorate when leakage, load, and pump dynamics change substantially. Fuzzy-based control has also been used in electro-hydraulic systems because it allows the controller gains to change according to the operating condition and helps in dealing with nonlinear behaviour and leakage effects [24]. Fractional-order control provides further flexibility by introducing fractional integral and derivative orders in addition to the conventional PID gains. Podlubny [27] introduced the FOPID controller, where λ and μ represent the fractional orders of integration and differentiation. These additional parameters make the controller more flexible, although the tuning process becomes more difficult [28]. In hydraulic systems, FOPID control has been applied to electro-hydraulic loading systems [25], and its practical performance has also been examined experimentally for hydraulically actuated systems [26]. Fuzzy fractional-order PID controllers have been studied for pressure-control applications [29] and hydraulic turbine governing systems [30]. More recently, fuzzy-FOPID control has also been tested experimentally for industrial hydraulic actuators [32]. These studies show that the combination of fuzzy logic and fractional-order control can be useful when the hydraulic system is nonlinear and its operating condition changes with time.

However, the selection of suitable proportional, integral, derivative, fractional-order, and fuzzy parameters is still a difficult task. Manual tuning becomes complicated when several objectives such as pressure tracking, flow regulation, ripple reduction, transient response, and actuator effort have to be considered together. Therefore, Harris Hawks Optimization (HHO), proposed by Heidari et al. [31], has been used in the present work to determine the controller parameters. HHO is a population-based optimization method in which the candidate solutions are updated through

exploration and exploitation stages. From the available literature, most radial piston pump studies have mainly focused on pump modelling, valve-plate design, efficiency improvement, and conventional pressure control [1–7]. Similarly, wear-related studies have mainly considered leakage behaviour, fault identification, and condition monitoring [17–20]. On the other hand, fuzzy and fractional-order controllers have mostly been applied to general electro-hydraulic systems [24–30,32]. Therefore, limited work has been reported on the combined study of piston-cylinder wear, leakage, pressure-flow deterioration, shaft-torque ripple, and HHO-tuned Fuzzy-FOPID control in a radial piston pump. This gap has motivated the present investigation.

The present work develops an HHO-tuned Fuzzy-FOPID strategy for coordinated pressure-flow regulation and shaft-torque-ripple reduction in a worn nine-piston radial piston pump. A nonlinear mathematical model has been formulated by considering piston kinematics, instantaneous delivery flow, pressure-dependent piston-cylinder leakage, manifold compressibility, load-flow behaviour, actuator dynamics, and shaft torque. Progressive wear has been introduced by increasing the radial clearance of one piston-cylinder pair while the remaining pairs have been kept healthy, allowing the progression from wear to leakage growth, pressure-flow degradation, and increased torque ripple to be quantified. The pump model has been implemented in MATLAB and validated against published radial-piston-pump pressure and flow results [3]. The controller has then been developed in two stages, with HHO used to tune the FOPID base parameters and the fuzzy supervisory scaling factors. The proposed controller has been compared with uncontrolled operation and HHO-tuned PID, FOPID, and Fuzzy-PID alternatives under the same operating conditions. In addition to pressure and flow tracking, the evaluation has included shaft-torque ripple, RMSE-based error reduction, actuator effort, and robustness over progressive wear levels. This formulation is intended to address the hydraulic and mechanical consequences of wear together rather than treating pressure regulation and pump degradation as separate problems.

The remaining paper is organized as follows. Section 1 introduces the research background. Section 2 presents the radial piston pump system description and mathematical modelling, including piston kinematics, leakage, pressure-flow dynamics, wear representation, and shaft-torque formulation. Section 3 presents the model-validation methodology. Moreover, section 4 describes the proposed Fuzzy-FOPID controller and the Harris Hawks Optimization-based parameter-tuning procedure. Section 5 discusses the wear-induced pump degradation and the comparative pressure, flow, torque-ripple, control-effort, and robustness results. Finally, Section 6 summarizes the main conclusions and outlines directions for future work.

2. System Description and Modelling

2.1 System Description

Figure 1 shows the hydraulic actuation and control arrangement considered for the pump system. The VDRPP is driven by an electric motor and connected to the hydraulic circuit through the suction and delivery lines. A hydraulic linear actuator is coupled to the pump displacement-control mechanism so that the pump operating condition can be adjusted through the directional control valve. The valve ports *P, T, A*, and *B* connect the pressure supply, tank, and the two actuator chambers, respectively. The spool motion of the valve is regulated through the control input supplied by the DAS and control unit. The pressure and control signals are acquired through the DAS and processed by the host computer for implementation of the proposed control strategy. The relief valve and filter are included to protect the hydraulic circuit and maintain the required oil condition during operation.

A detailed view of the radial piston pump has been shown in Fig. 2. The pump consists of a cylinder block, radial pistons, cam ring, drive shaft, suction port, and delivery port. The pistons are arranged circumferentially around the cylinder block and reciprocate radially as the shaft rotates. During the suction phase, the piston chamber communicates with the low-pressure suction port, whereas during the delivery phase the compressed fluid is discharged through the high-pressure delivery port. The suction and delivery regions are separated by the port arrangement, and the angular position of each piston determines its instantaneous pumping contribution. The cam ring governs the radial displacement of the pistons and hence the instantaneous pump flow. In the present study, the detailed radial piston arrangement has been used for developing the mathematical model of piston kinematics, leakage, delivery pressure, flow rate, and shaft-torque characteristics under healthy and worn operating conditions.

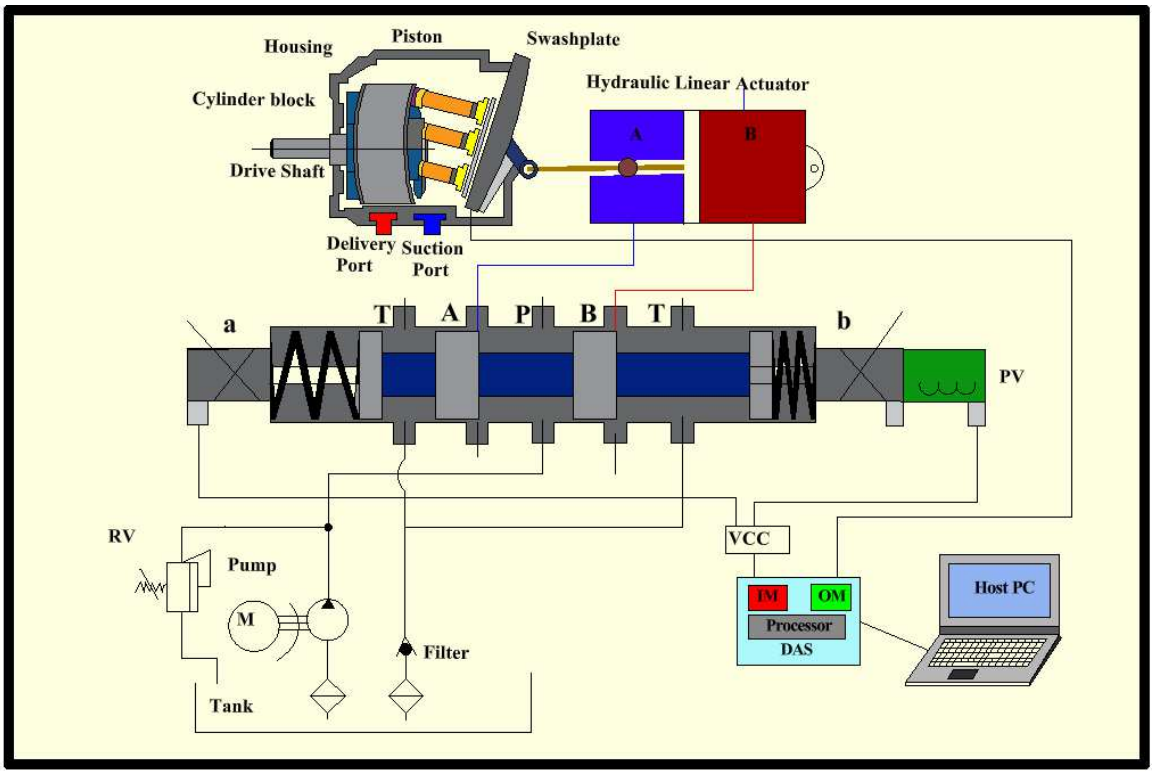


Fig. 1. Schematic arrangement of the hydraulic actuation and control system used for pump displacement regulation.

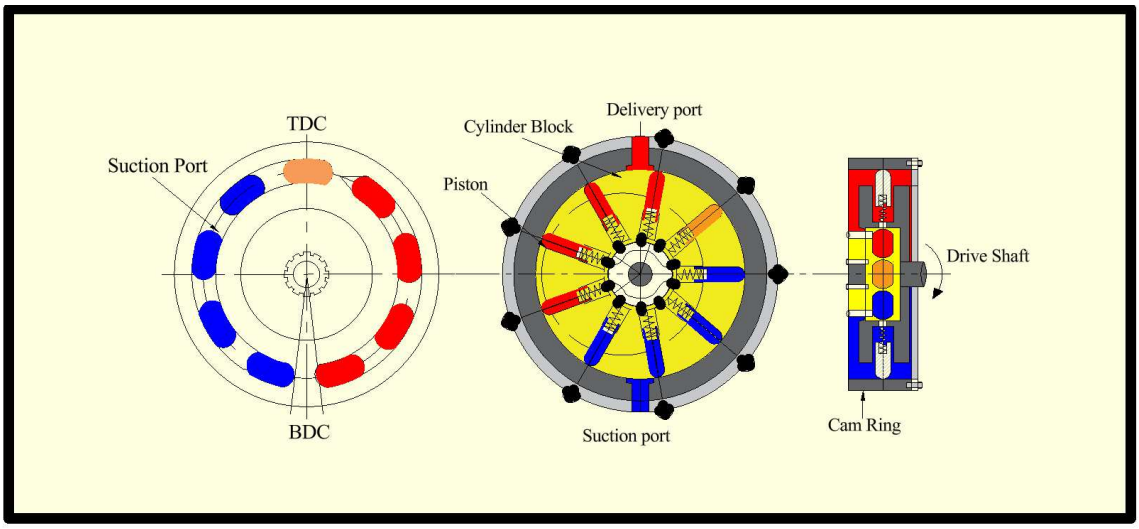


Fig. 2. Detailed schematic representation of the radial piston pump showing the suction and delivery ports, cylinder block, radial pistons, cam ring, and drive shaft.

2.2 Mathematical Modelling

The system considered in the present study is a nine-piston radial piston pump connected to a hydraulic load. The pump mainly consists of a cylinder block (rotor), nine equally spaced pistons, a cam ring (stator), drive shaft, suction port and delivery port. The shaft rotates at a constant speed and the eccentricity between the rotor and cam ring produces the reciprocating motion of the pistons. During one revolution, each piston passes through suction and delivery phases and

contributes periodically to the total pump flow. The suction side has been maintained at $P_s = 0.20$ MPa, whereas the nominal delivery-pressure operating point has been taken as $P_nom = 10.04$ MPa.

Piston-cylinder wear has been introduced in one piston-cylinder pair, while the remaining eight pairs have been kept healthy. The healthy radial clearance is $h_0 = 16$ μm and the worn clearance has been increased up to 32 μm. The increase in clearance produces additional internal leakage, which directly influences the delivery pressure, output flow and shaft-torque fluctuation. The controller acts through the normalized pump command $u(t)$, and the same nonlinear pump model has been used for the wear analysis, controller tuning and all reported MATLAB simulations.

2.2.1 Piston kinematics and instantaneous delivery flow

For the ith piston, the angular position has been written by considering equal angular spacing among the nine pistons as

$$\theta_i(t) = \omega t + \frac{2\pi(i-1)}{z} \tag{1}$$

where z is the number of pistons and ω is the shaft angular speed. The angular speed is obtained from the rotational speed n as

$$\omega = \frac{2\pi n}{60} \tag{2}$$

The radial displacement of a piston has been represented by the eccentric kinematic relation including the second-harmonic correction as

$$x_i(\theta_i) = e(1 - \cos\theta_i) + \frac{e^2}{4r_s}(1 - \cos 2\theta_i) \tag{3}$$

Differentiating Eq. (3) with respect to the piston angle gives

$$\frac{\mathrm{d}x_i}{\mathrm{d}\theta_i} = e[\sin\theta_i + \frac{e}{2r_s}\sin 2\theta_i] \tag{4}$$

$$\dot{x}_i = \omega\frac{\mathrm{d}x_i}{\mathrm{d}\theta_i} \tag{5}$$

The instantaneous kinematic flow generated by the ith piston is therefore

$$q_i = A_p\dot{x}_i \tag{6}$$

Only the piston delivering fluid to the high-pressure side contributes to the positive delivery flow. Hence, the effective contribution of each piston and the total kinematic delivery flow are written as

$$q_{i,d} = \max(q_i, 0) \tag{7}$$

$$q_{kin} = \sum_{i=1}^{z} q_{i,d} \tag{8}$$

For the present radial configuration, the theoretical displacement per revolution is

$$V_d = 2zA_p e \tag{9}$$

2.2.2 Piston-cylinder wear and internal leakage

The piston-cylinder clearance has been selected as the wear-sensitive parameter. In the present model, piston 1 has been considered as the worn pair and the remaining pistons have been maintained at the healthy clearance. The worn and healthy clearances are expressed as

$$h_1 = \gamma h_0 \tag{10}$$

$$h_i = h_0, \;\; i = 2, 3, \ldots, z \tag{11}$$

The corresponding percentage wear and the wear multipliers used in the simulation have been defined by

$$W = 100(\gamma - 1)\% \tag{12}$$

$$\gamma \in \{1.00, 1.25, 1.50, 1.75, 2.00\} \tag{13}$$

The leakage between the piston and cylinder has been represented by the laminar annular-clearance relation. The leakage coefficient of each piston-cylinder pair is

$$C_i = \frac{\pi d_p {h_i}^3}{12\mu L_{pc}} \tag{14}$$

Since leakage is considered only when a piston is connected to the delivery side, an activation function has been used as

$$\chi_i(\mathrm{t}) = \mathrm{H}(q_i);\ \mathrm{H} = 1 \text{ for } q_i \geq 0,\quad \mathrm{H} = 0 \text{ otherwise} \tag{15}$$

$$C_{active}(\mathrm{t} = \sum_{i=1}^{z} \chi_i(t) C_i \tag{16}$$

The instantaneous pressure difference across the pump and the total piston-cylinder leakage are therefore

$$\Delta P(\mathrm{t}) = P_d(\mathrm{t}) - P_s \tag{17}$$

$$Q_{leak}(\mathrm{t}) = C_{active}(t)\, \Delta P(t) \tag{18}$$

Equation (14) shows the cubic dependence of leakage on the radial clearance. Thus, even a moderate increase in clearance can produce a noticeable rise in internal leakage. This relation has been retained directly in the MATLAB model used for the progressive-wear results.

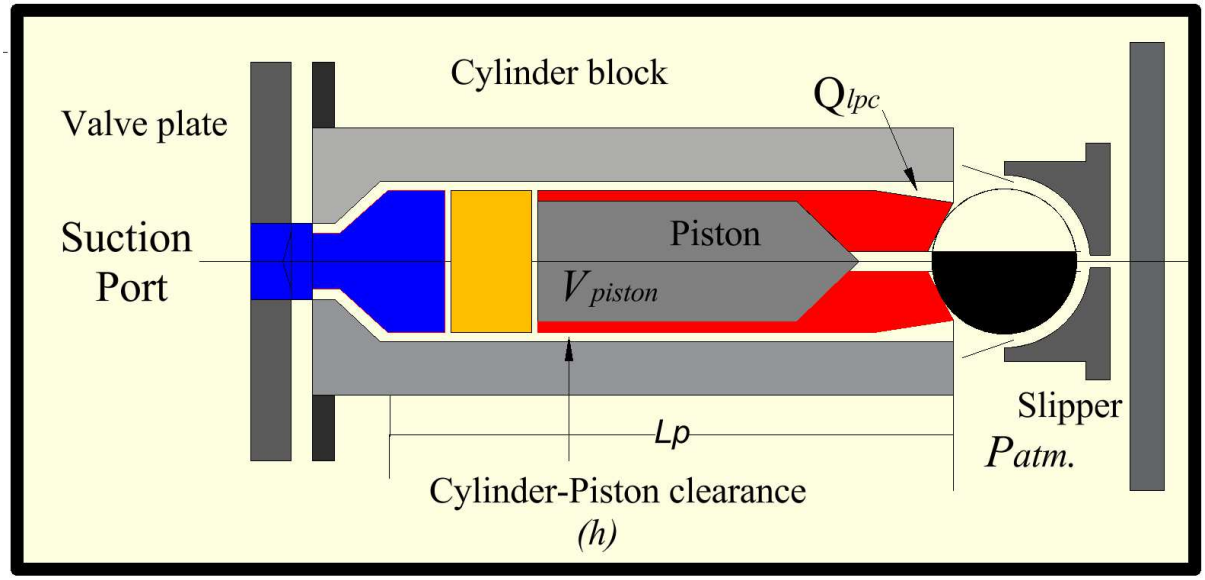


Fig. 3. Schematic representation of the piston–cylinder pair of the radial piston pump showing the internal leakage path through the piston–cylinder clearance

Figure 3 shows the schematic representation of a single piston–cylinder pair of the radial piston pump considered in the present study. The piston reciprocates inside the cylinder block, while the valve plate provides communication with the suction port. The small radial clearance *h* between the piston and cylinder wall forms an internal leakage path, represented by *Qlpc*. The effective leakage length is denoted by *Lp,* while *Vpiston* represents the instantaneous piston-chamber volume. During normal operation, the clearance remains small; however, progressive piston–cylinder wear increases *h*, resulting in a higher leakage flow through the annular clearance. This leakage reduces the effective pump delivery and consequently affects the outlet pressure, flow rate, and shaft-torque characteristics. In the present model, the variation of *h* has therefore been used to represent different levels of piston–cylinder wear.

2.2.3 Pump delivery, hydraulic load and pressure dynamics

The normalized actuator command *u(t)* changes the effective pump delivery. After subtracting the internal leakage, the net pump flow supplied to the delivery manifold is expressed as

$$Q_{pump}(\mathrm{t}) = u(t)\, q_{kin}(\mathrm{t}) - Q_{leak}(t) \tag{19}$$

The hydraulic load has been represented by a square-root pressure-flow relationship as

$$Q_L(\mathrm{t}) = K_L\sqrt{\Delta P(t)} \tag{20}$$

The load coefficient has been calibrated using the healthy pump at the nominal pressure of 10.04 MPa. Hence,

$$K_L = \frac{\bar{q}_{kin,0} - C_{active,0}(P_{nom} - P_s)}{\sqrt{P_{nom} - P_s}} \tag{21}$$

where the overbar denotes the mean value over one complete shaft revolution for the healthy pump. With the present parameters, the calibrated load coefficient is approximately $K_L = 8.8493\times10^{-7}$ m³/(s√Pa). The pressure dynamics in the delivery manifold are obtained from the fluid continuity relation as

$$\frac{\mathrm{d}P_d}{\mathrm{d}t} = \frac{\beta}{V_{man}}[Q_{pump}(\mathrm{t}) - Q_L(\mathrm{t})] \tag{22}$$

The delivered flow used for the pressure-flow results is the load flow leaving the delivery manifold, i.e.,

$$Q_{out}(\mathrm{t}) = Q_L(t) \tag{23}$$

2.2.4 Shaft-torque formulation and ripple index

The shaft-torque signal has been evaluated from the instantaneous pressure rise and the controlled kinematic pump flow. This definition has been used consistently in the torque-ripple and controller-comparison results and is expressed as

$$T_s(\mathrm{t}) = \frac{\Delta P(t)\, u(t)\, q_{kin}(t)}{\omega} \tag{24}$$

For a generic periodic output X representing delivery pressure, output flow or shaft torque, the ripple percentage has been calculated over the selected steady-state interval as

$$R_X = \frac{X_{max} - X_{min}}{X} \times 100\%, \quad X \in \{P_d, Q_{out}, T_s\} \tag{25}$$

2.2.5 Actuator dynamics and reference demand

The control action has been introduced through a first-order displacement/flow-control actuator. This block corresponds to the actuator shown in the control-system diagram and avoids assuming an instantaneous change in pump command. The actuator dynamics and physical limits are

$$\tau_{act}\frac{\mathrm{d}u}{\mathrm{d}t} + u(\mathrm{t}) = \mathrm{sat}[u_{cmd}(\mathrm{t})], \quad u_{min} \le u(\mathrm{t}) \le u_{max} \tag{26}$$

In the present simulations, τ_act = 1.2 ms, u_min = 0.80 and u_max = 1.25. For the step-response comparison, the same pressure demand has been applied to all controllers and wear conditions. The pressure, flow and torque reference quantities are

$$P_d^*(\mathrm{t}) = 9.29\ \mathrm{MPa}\ \text{for}\ t < 1\ \mathrm{s};\quad 10.79\ \mathrm{MPa}\ \text{for}\ t \geq 1\ \mathrm{s} \tag{27a}$$

$$T_s^*(\mathrm{t}) = \frac{(P_d^*(\mathrm{t}) - P_s)V_d}{2\pi} T_s^*(\mathrm{t}) = \frac{(P_d^*(\mathrm{t}) - P_s)V_d}{2\pi} \tag{27b}$$

$$T_s^*(\mathrm{t}) = \frac{(P_d^*(\mathrm{t}) - P_s)V_d}{2\pi} \tag{27c}$$

With the calibrated load relation, the step pressure demand corresponds to an output-flow demand of approximately 160.08 to 172.78 L/min and a theoretical torque demand of approximately 165.93 to 193.31 N·m. These same reference conditions have been retained in the pressure, flow, torque, control-effort and progressive-wear results.

The principal pump, fluid, wear and actuator parameters used in the MATLAB simulations are summarized in Table 1. The same values have been retained throughout the wear analysis and controller evaluation.

Table 1. Simulation parameters of the radial piston pump model.

Symbol	Description	Value
z	Number of pistons	9
n	Rotational speed	1500 rpm
ω	Angular speed	157.08 rad/s
e	Eccentricity	0.012 m
r_s	Cam/stroking-ring radius	0.10 m
A_p	Piston area	5.31×10^{-4} m²
d_p	Piston diameter	0.026 m
P_s	Suction pressure	0.20 MPa
P_{nom}	Nominal delivery pressure	10.04 MPa
μ	Dynamic viscosity of oil	0.05622 Pa·s
β	Effective bulk modulus	845.7 MPa
V_{man}	Delivery-manifold volume	3.0×10^{-4} m³
L_{pc}	Piston-cylinder leakage path length	0.24 mm
h_0	Healthy radial clearance	16 μm
h_w	Worn radial clearance	20, 24, 28, 32 μm
K_L	Hydraulic-load coefficient	8.8493×10^{-7} m³·s⁻¹·Pa⁻¹ᐟ²
τ_{act}	Actuator time constant	1.2 ms
u_{min}, u_{max}	Normalized command limits	0.80, 1.25
Δt	Time step for controller simulations	1.0×10^{-4} s

The above formulation provides the nonlinear plant model used in the present work. It preserves the physical link between piston-cylinder wear, leakage growth, delivery-pressure and flow degradation, and shaft-torque fluctuation. Therefore, the controller design presented in the

following section has been evaluated against the same model rather than against a simplified independent plant.

3. Validation

The developed radial piston pump model has been validated with the published results of Mandal et al. (2022). For validation, the same five-piston pump configuration and operating conditions have been considered in the present simulation. The delivery pressure and flow responses have been compared over the complete angle of rotation, and the corresponding error profiles have also been evaluated. The close agreement between the present simulation and the reported results has confirmed the accuracy of the developed model and has provided a reliable basis for further analysis under worn-pump conditions and for evaluating the proposed controller performance.

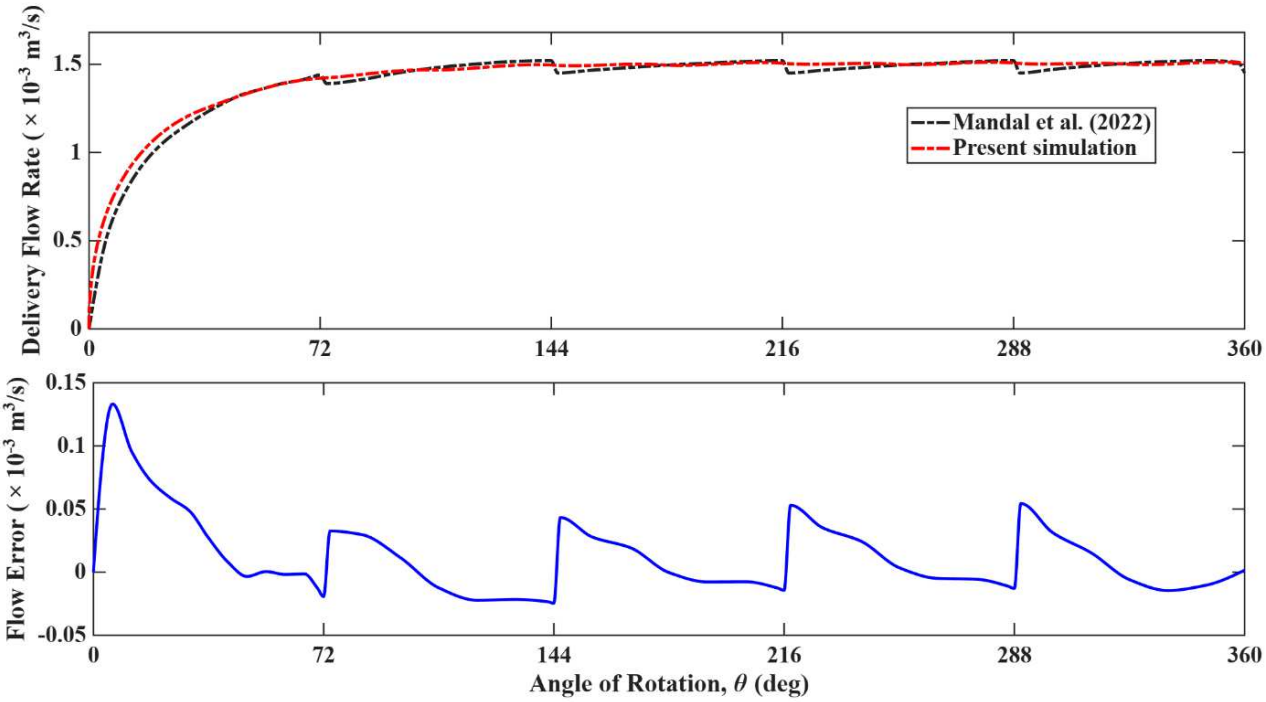


Fig. 4. Validation of the five-piston radial piston pump delivery pressure: (a) comparison of Mandal et al. (2022) and the present simulation with respect to angle of rotation; (b) corresponding pressure error.

Figure 4(a) shows the validation of delivery pressure for the five-piston radial piston pump. The present simulation closely follows the result reported by Mandal et al. (2022) over the complete angle of rotation. The present model gives a mean pressure of 10.0135 MPa compared to 10.04 MPa reported in the literature, with an error of only 0.2644%. The corresponding pressure error is shown in Fig. 4(b), which confirms good agreement between the two results.

Similarly, Fig. 5(a) shows the comparison of delivery flow with Mandal et al. (2022). The present model gives a mean flow of 90.2353 L/min compared to the reported value of 90 L/min, resulting in an error of about 0.2614%. The corresponding flow error is shown in Fig. 5(b). The close

agreement in both pressure and flow confirms the validity of the developed five-piston pump model for further analysis of the proposed worn pump system.

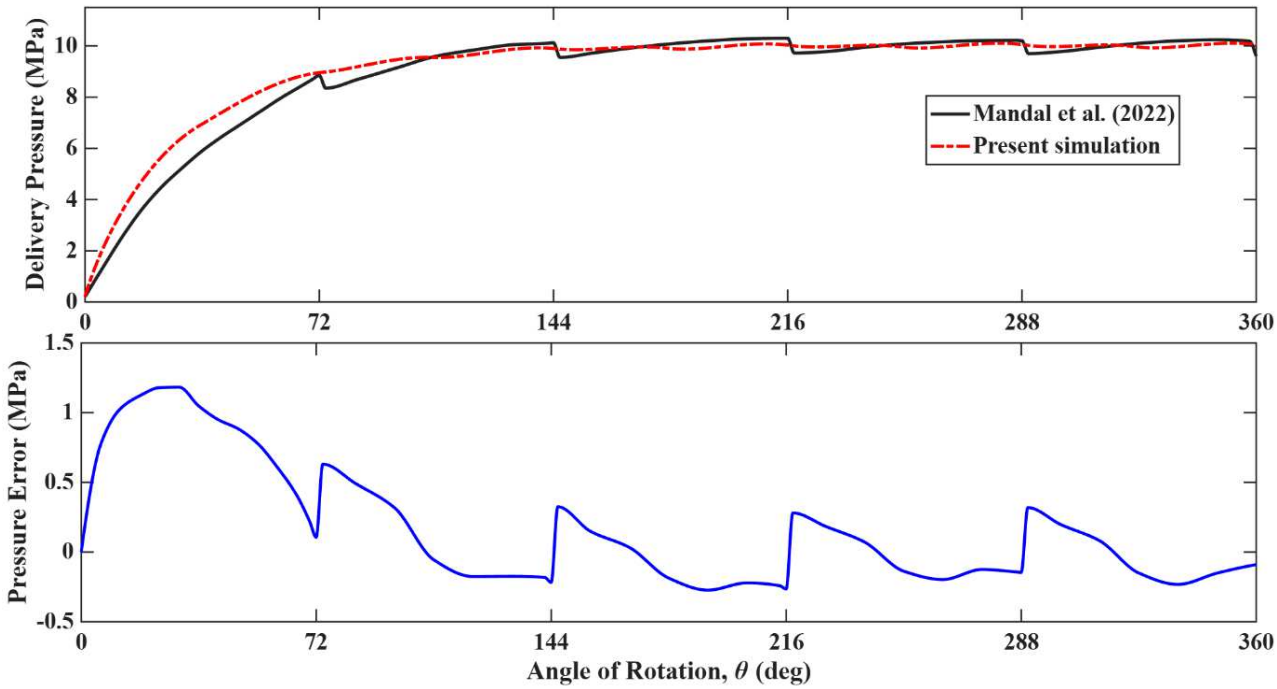


Fig. 5. Validation of the five-piston radial piston pump delivery flow: (a) comparison of Mandal et al. (2022) and the present simulation with respect to angle of rotation; (b) corresponding flow error.

Table 2. Validation of the present piston radial piston pump model against Mandal et al. (2022).

Quantity	**Mandal et al. (2022)**	**Present model**	**Error (%)**
Delivery pressure	10.0400 MPa	10.0135 MPa	0.2644%
Delivery flow	90.0000 L/min	90.2353 L/min	0.2614%

The five-piston radial piston pump model has been validated against the results reported by Mandal et al. (2022). The present simulation predicted a mean delivery pressure of 10.0135 MPa compared with the reference value of 10.04 MPa, corresponding to an error of 0.2644%. Similarly, the predicted delivery flow was 90.2353 L/min compared with the reported value of 90 L/min, giving an error of 0.2614%. The close agreement supports the adequacy of the reproduced baseline model for subsequent extension to the worn nine-piston pump configuration.

4. Controller Design

The control scheme has been developed to maintain the delivery pressure of the nine-piston radial piston pump while reducing the associated flow deterioration and shaft-torque fluctuation caused by piston-cylinder wear. A fractional-order PID (FOPID) controller has been combined with a fuzzy supervisory mechanism and Harris Hawks Optimization (HHO). The fractional orders

provide additional flexibility compared with a conventional PID controller, whereas the fuzzy supervisor adjusts the effective controller gains according to the instantaneous tracking condition. HHO has been employed to tune the controller parameters using a multi-objective index that accounts for pressure tracking, flow regulation, and torque-ripple suppression. The controller design has been formulated in the same concise progression generally adopted in the authors' earlier electrohydraulic control work, but it has been reformulated here for the worn radial piston pump and the present pressure-flow-torque objective.

In the proposed architecture, the delivery pressure is used as the real-time feedback variable. The flow and shaft torque are coupled to the pressure response through the nonlinear pump model and are included explicitly in the HHO objective function. Hence, a single bounded actuator command has been tuned to obtain pressure regulation without producing excessive flow ripple or shaft-torque oscillation.

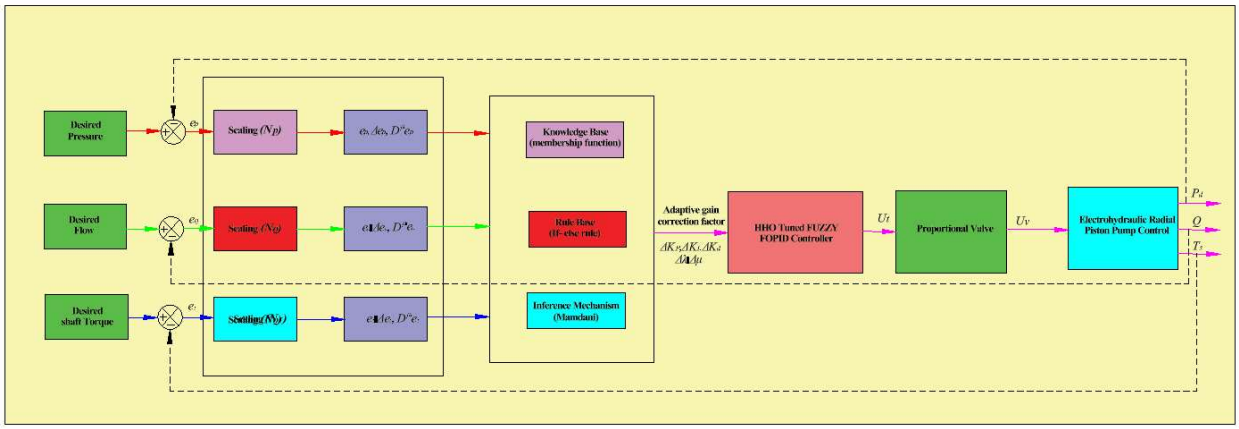


Fig. 6. Proposed HHO-tuned Fuzzy-FOPID control architecture for coordinated pressure-flow regulation and shaft-torque-ripple suppression in the worn radial piston pump.

Figure 6 illustrates the proposed HHO-tuned Fuzzy-FOPID control architecture used for the worn radial piston pump. The delivery-pressure error is processed by the fuzzy supervisory FOPID controller, while HHO is employed offline to determine the optimal controller gains, fractional orders, and fuzzy scaling parameters. The actuator command is then applied to the nonlinear pump model, where piston-cylinder wear, load variation, and pressure disturbances are considered. The resulting pressure, flow, and shaft-torque responses are used to evaluate the controller performance. This structure allows the proposed controller to maintain pressure-flow regulation while simultaneously reducing wear-induced torque fluctuation, thereby supporting the main objective of the present study.

Let $P_{ref}(t)$ be the required delivery pressure and $P(t)$ be the instantaneous pump delivery pressure. The normalized pressure error and its rate have been defined as

$$e(t) = \frac{P_{ref}(t) - P(t)}{P_{ref}(t)} \tag{28}$$

$$\dot{e}(t) = \frac{de(t)}{dt} \tag{29}$$

The normalized form has been selected so that the controller input remains dimensionless over the investigated operating range. The nominal pressure used during controller optimization has been 10.04 MPa. After tuning, the same controller parameters have been retained for the step-demand variation from 9.29 to 10.79 MPa and for all wear conditions from the healthy state to 100% wear. No wear-dependent retuning has been applied during the final robustness assessment.

A conventional PID controller uses fixed proportional, integral, and derivative actions. For the nonlinear and wear-dependent pump dynamics, a fractional-order $PI^{\lambda} D^{\mu}$ structure has been adopted [27,28]. The baseline control signal can be expressed as,

$$u_{FO}(t) = 1 + K_p e(t) + K_i D_t^{-\lambda} e(t) + K_d D_t^{\mu} e(t) \tag{30}$$

where K_p, K_i, and K_d are the proportional, integral, and derivative gains, respectively; λ is the fractional integral order and μ is the fractional derivative order. The unity term represents the nominal pump command. For $\lambda = \mu = 1$, the controller reduces to the conventional PID form. The fractional operators have been evaluated using the Grünwald-Letnikov (GL) approximation, written as,

$$D_t^{\alpha} e(t_k) \approx \Delta t^{-\alpha} \sum_{j=0}^{M} w_j^{(\alpha)} e(t_{k-j}) \tag{31}$$

$$w_0^{(\alpha)} = 1, \; w_j^{(\alpha)} = [1 - \frac{\alpha + 1}{j}] w_{j-1}^{(\alpha)} \tag{32}$$

where Δt is the sampling interval and M is the finite memory length. In the present formulation, $\alpha = -\lambda$ has been used for fractional integration and $\alpha = \mu$ for fractional differentiation. This finite-memory implementation retains the recent error history required for the pump transient while keeping the computational burden within a practical range.

The FOPID controller improves tuning flexibility; however, a fixed gain set cannot fully represent the change in pump behavior as the piston-cylinder clearance increases. Therefore, a fuzzy supervisory layer has been introduced to adapt the effective proportional, integral, and derivative gains while retaining the optimized fractional orders. The magnitudes of the normalized pressure error and filtered error rate are used as the fuzzy inputs. The normalized fuzzy variables are defined as,

$$E = min\{\frac{|e|}{s_e}, 1\}, \quad \Delta E = min\{\frac{\left|\frac{d\,e}{d\,t}\right|}{s_{\Delta e}}, 1\} \tag{33}$$

where s_e and $s_{\Delta e}$ are the HHO-tuned scaling parameters. Both fuzzy inputs are limited to the interval [0,1] and are represented by Low (L), Medium (M), and High (H) triangular membership functions. These functions are given by

$$\mu_L(x) = \max\{0, \min[1, \frac{0.5 - x}{0.5}]\} \tag{34}$$

$$\mu_M(x) = \max\{0, 1 - \frac{|x - 0.5|}{0.5}\} \tag{35}$$

$$\mu_H(x) = \max\{0, \min[1, \frac{x - 0.5}{0.5}]\} \tag{36}$$

For each combination of E and ΔE, product inference and normalized weighted averaging are used to obtain the proportional, integral, and derivative gain factors. The rule contribution is evaluated from $W_{ij} = \mu_i(E)\mu_j(\Delta E)$. The gain-factor matrices used in the present controller are listed in Table 3. The proportional and derivative actions are increased when the tracking deviation becomes large, whereas the integral action is reduced at large error and error rate to limit integral accumulation during the transient.

Table 3. Fuzzy supervisory gain-factor matrices used in the proposed controller.

Gain factor	**E**	**ΔE = L**	**ΔE = M**	**ΔE = H**
f_p	L	0.85	1.00	1.15
f_p	M	1.05	1.20	1.35
f_p	H	1.25	1.45	1.65
f_i	L	1.15	1.00	0.85
f_i	M	1.05	0.90	0.75
f_i	H	0.85	0.70	0.55
f_d	L	0.80	1.00	1.25
f_d	M	0.90	1.15	1.40
f_d	H	1.00	1.30	1.60

The fuzzy outputs are not applied directly to the actuator. Instead, the HHO-tuned supervisory strengths η_p, η_i, and η_d determine the amount by which the fuzzy gain factors modify the optimized FOPID gains. The adaptive gains are therefore obtained as

$$K_p{}^*(t) = K_{p0}\,[1 + \eta_p(f_p - 1)] \tag{37}$$

$$K_i{}^*(t) = K_{i0}\,[1 + \eta_i(f_i - 1)] \tag{38}$$

$$K_d{}^*(t) = K_{d0}\,[1 + \eta_d(f_d - 1)] \tag{39}$$

where K_{p0}, K_{i0}, and K_{d0} are the optimized baseline FOPID gains. When $\eta_p = \eta_i = \eta_d = 0$, the structure becomes the optimized FOPID controller. The non-zero supervisory strengths introduce only the gain variation required by the HHO solution. The final HHO-Fuzzy-FOPID command is obtained by substituting the adaptive gains in Eq. (30).

The controller output has been restricted to the admissible actuator range so that the reported performance is not obtained through unrealistic control action. The command saturation and first-order actuator dynamics are represented by

$$u_{cmd}(t) = \text{sat}[u_{FFOPID}(t), u_{min}, u_{max}] \tag{40}$$

$$\tau_a \frac{d\,u(t)}{d\,t} + u(t) = u_{cmd}(t) \tag{41}$$

In the present study, $u_{min} = 0.80, u_{max} = 1.25$ and $\tau_a = 1.2\ ms$. These limits have been imposed during both optimization and final simulation. The subsequent control-effort results have confirmed bounded operation without actuator saturation under the severe-wear step test.

The enlarged FOPID-fuzzy parameter space makes manual tuning difficult because improving pressure tracking can simultaneously increase flow ripple, shaft-torque fluctuation, or control effort. Therefore, HHO has been employed to obtain the controller parameters [31]. In HHO, each hawk represents a candidate solution and the best candidate represents the prey. The transition between exploration and exploitation is governed by the escaping-energy parameter

$$E_H(t) = 2E_0(1 - \frac{t}{T}),\ \ E_0 = 2r - 1,\ \ r \in [0,1] \tag{42}$$

where t and T are the current and maximum iterations, respectively. When the magnitude of E_H is greater than or equal to 1, the hawks explore different regions of the search space; when its magnitude is less than 1, the exploitation stage is activated through the soft/hard besiege and rapid-dive mechanisms. After each update, the candidate variables are returned to their prescribed limits.

A two-stage optimization procedure has been adopted. In Stage 1, the baseline FOPID vector $x_{FO} = [K_p, K_i, K_d, \lambda, \mu]$ is optimized over the complete wear range. The wear cases 0%, 25%, 50%, 75%, and 100% are assigned the weights 0.10, 0.15, 0.20, 0.25, and 0.30, respectively. Thus, the higher wear levels receive greater importance without sacrificing healthy-condition performance. The Stage-1 objective is written as,

$$J_1 = \sum_{m=1}^{5} w_m J_m \tag{43}$$

$$J_m = 0.28\frac{\text{RMSE}_P{}^2}{0.50} + 0.14\frac{\text{RMSE}_Q{}^2}{4.00} + 0.14\frac{R_P{}^2}{8.00} + 0.09\frac{R_Q{}^2}{4.00} \tag{44}$$

$$+ 0.27\frac{R_T}{12.0}^2 + 0.03\frac{M_p}{2.00}^2 + 0.05\frac{t_s}{0.08}^2$$

Here RMSE_P and RMSE_Q are the pressure and flow root-mean-square errors; R_P, R_Q, and R_T are the pressure, flow, and shaft-torque ripple percentages; M_p is the pressure overshoot; and t_s is the settling time. The normalizing constants place the different performance quantities on comparable scales.

In Stage 2, the optimized FOPID base is retained and HHO determines the fuzzy supervisory vector $z = [s_e, s_{\Delta e}, \eta_p, \eta_i, \eta_d]$. This stage has been performed at the limiting 100% wear condition because the supervisor is required primarily to preserve regulation when leakage and torque disturbance are most severe. The objective function is defined as

$$J_2 = 0.58\frac{R_T}{3.0}^2 + 0.12\frac{R_P}{4.0}^2 + 0.06\frac{R_Q}{2.0}^2 + 0.12\frac{\mathrm{RMSE}_P}{0.18}^2 + 0.06\frac{\mathrm{RMSE}_Q}{1.50}^2 + 0.06\frac{\overline{P} - 10.04}{0.15}^2 \quad (45)$$

The largest weight in Eq. (45) has been assigned to R_T because shaft-torque-ripple suppression is one of the central objectives of the present work. The pressure and flow terms simultaneously prevent the mechanical improvement from being obtained at the expense of hydraulic regulation. The final solution is validated using the full-resolution nonlinear pump model, and the same optimized controller is retained for all controller-comparison and progressive-wear tests. The decision-variable limits have been selected to provide a sufficiently broad search region while preventing unrealistic controller gains and fractional orders. The optimized parameters used in the final MATLAB simulations are listed in Table 4.

Table 4. Search bounds and optimized parameters of the HHO-Fuzzy-FOPID controller.

Stage	Parameter	Description	Search range	Optimized value
Stage 1	$\boldsymbol{K_p}$	Proportional gain	0.05–4.00	0.833307
Stage 1	$\boldsymbol{K_i}$	Integral gain	0.50–60.00	53.969547
Stage 1	$\boldsymbol{K_d}$	Derivative gain	0–0.006	0.003955
Stage 1	$\boldsymbol{\lambda}$	Fractional integral order	0.55–1.00	0.939237
Stage 1	$\boldsymbol{\mu}$	Fractional derivative order	0.50–1.00	0.830034
Stage 2	$\boldsymbol{s_e}$	Error scaling factor	0.005–0.080	0.006344
Stage 2	$\boldsymbol{s_{\Delta e}}$	Error-rate scaling factor	2.0–30.0	7.352926
Stage 2	$\boldsymbol{\eta_p}$	Fuzzy P adaptation strength	0–1	0.074580
Stage 2	$\boldsymbol{\eta_i}$	Fuzzy I adaptation strength	0–1	0.092079
Stage 2	$\boldsymbol{\eta_d}$	Fuzzy D adaptation strength	0–1	0.092950

The optimized fractional orders $\lambda = 0.9392$ and $\mu = 0.8300$ show that the best solution has not been obtained by forcing the controller to an integer-order PID structure. In addition, the non-zero supervisory strengths indicate that a moderate fuzzy adaptation of the baseline gains is useful, while their relatively small values avoid aggressive gain variation. This behaviour is consistent with the bounded actuator effort obtained in the severe-wear simulations.

5. Results and Discussion

The mean leakage has increased from approximately 5.49 L/min under the healthy condition to 9.19 L/min at 100% wear**,** corresponding to an increase of about 67.4%**.** Similarly, the peak leakage has increased from about 6.11 L/min to 14.67 L/min**.** The periodic variation in leakage with the angle of rotation has occurred due to the successive delivery action of the pistons during each shaft revolution. The increase in clearance due to wear has provided a larger leakage path for the hydraulic fluid, which has resulted in significantly higher leakage under severe wear conditions. Thus, the result clearly demonstrates that progressive piston-cylinder wear has a strong influence on the internal leakage characteristics of the radial piston pump and provides the basis for further investigation of its effect on delivery pressure, flow rate, and torque ripple**.**

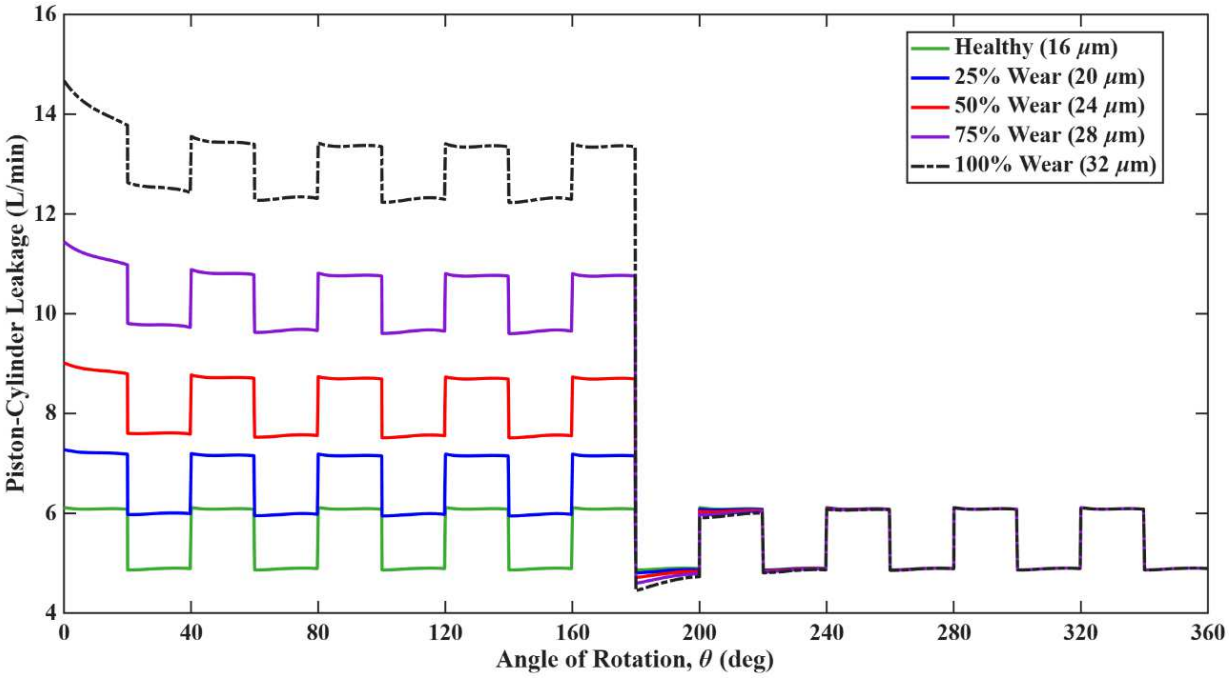


Fig. 7. Effect of progressive piston-cylinder wear on the instantaneous leakage characteristics of the nine-piston radial piston pump.

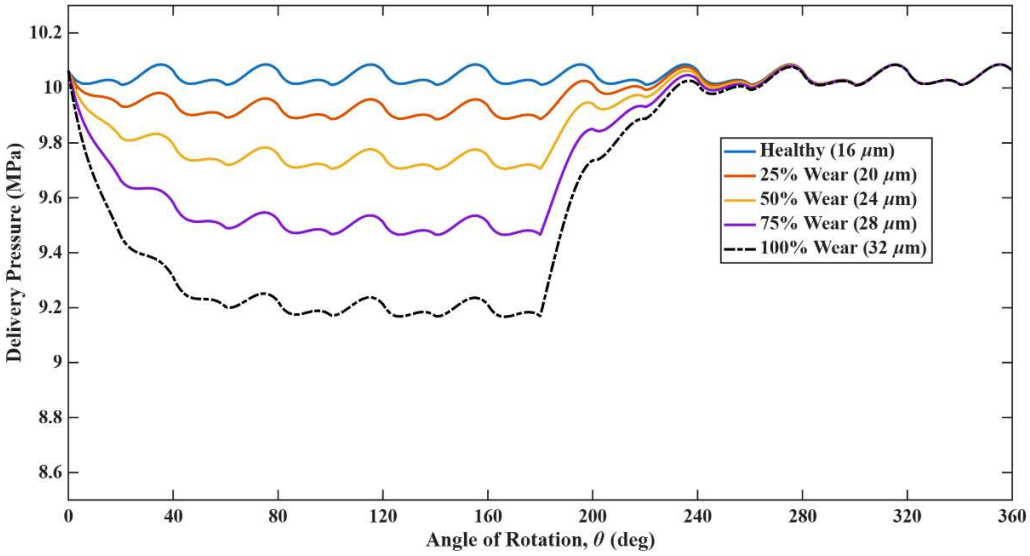


Fig. 8. Effect of progressive piston-cylinder wear on the delivery-pressure characteristics of the nine-piston radial piston pump over one complete shaft revolution.

Figure 9 shows the effect of progressive piston-cylinder wear on the delivery pressure of the nine-piston radial piston pump. The delivery pressure decreases progressively as the clearance increases, while the pressure oscillation becomes more pronounced. The pressure ripple rises from approximately 0.73% in the healthy condition to about 9.55% at 100% wear. This trend is consistent with the cubic clearance-dependent leakage relation, since the larger leakage path reduces the effective delivery of the worn piston during the high-pressure stroke. The result therefore establishes the direct hydraulic consequence of piston-cylinder wear before evaluating the proposed controller.

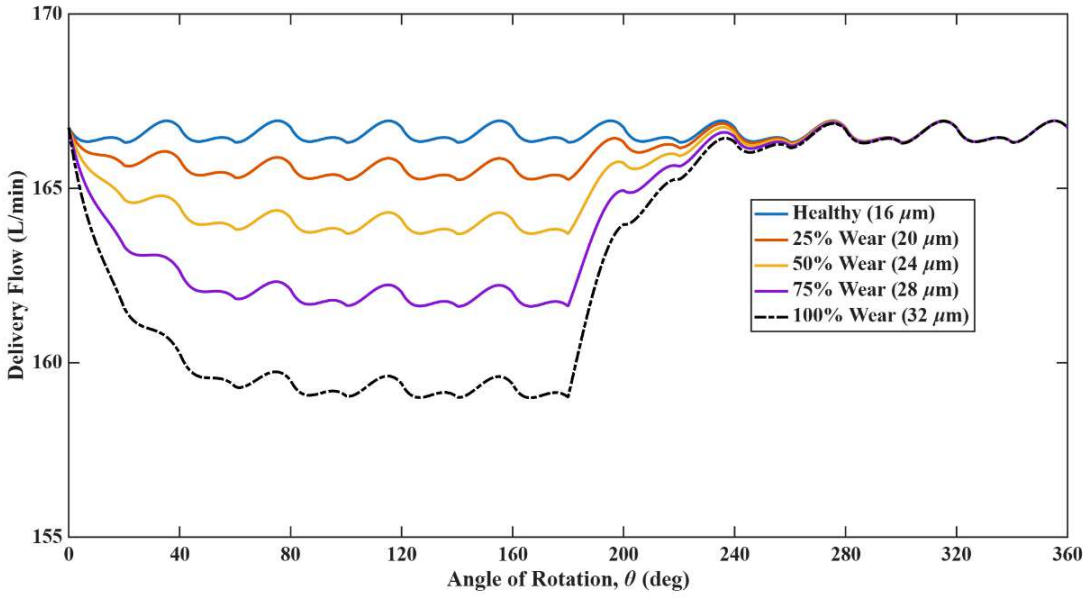


Fig. 9. Effect of progressive piston-cylinder wear on the delivery-flow characteristics of the nine-piston radial piston pump over one complete shaft revolution.

Figure 9 shows the effect of progressive piston-cylinder wear on the delivery flow of the nine-piston radial piston pump. In continuation of the previous results, the increase in leakage observed in Fig. 7 and the reduction in delivery pressure observed in Fig. 8 are reflected here in the form of degraded flow performance. It is observed that the delivery flow decreases gradually as the wear level increases from healthy condition to 100% wear.

Table 5. Numerical delivery-flow values under healthy and worn piston-cylinder conditions.

Condition	Clearance (μm)	Mean flow (L/min)	Min. flow (L/min)	Max. flow (L/min)	Flow ripple (%)	Mean flow reduction (%)
Healthy	16	90.0153	89.8472	90.1830	0.3730	0.0000
25% Wear	20	89.7240	89.2672	90.1811	1.0188	0.3237
50% Wear	24	89.3013	88.4250	90.1778	1.9628	0.7933
75% Wear	28	88.7339	87.2972	90.1728	3.2393	1.4238
100% Wear	32	88.0157	85.8702	90.1657	4.8761	2.2213

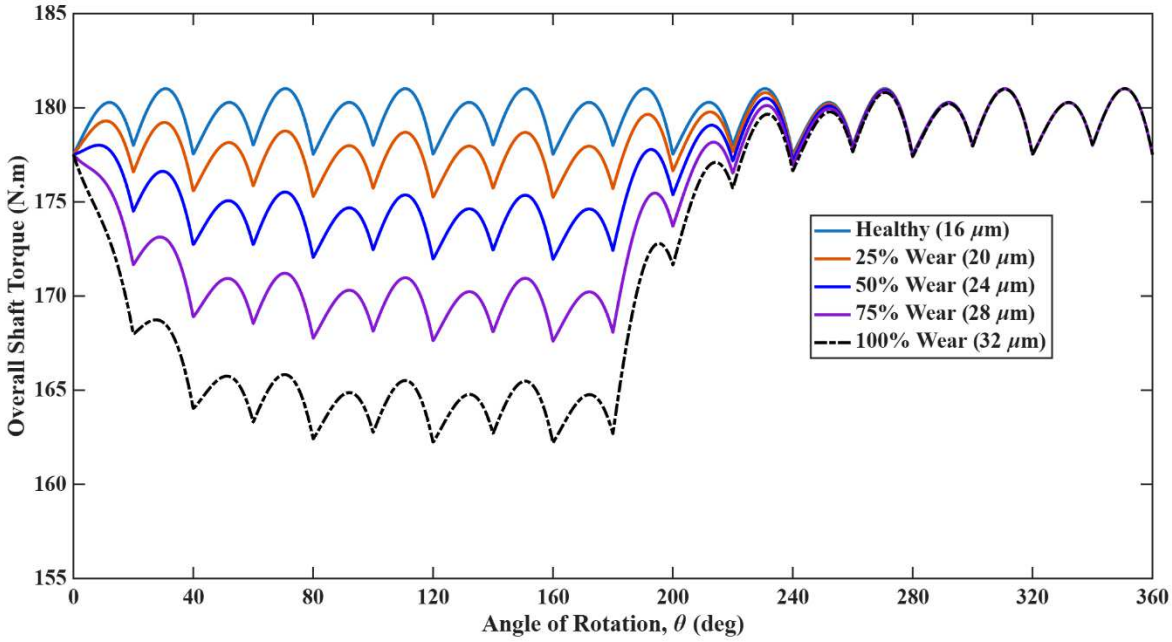


Fig. 10. Effect of progressive piston-cylinder wear on the shaft-torque characteristics of the nine-piston radial piston pump over one complete shaft revolution.

The mean delivery flow decreases from about 90.02 L/min in the healthy case to 88.02 L/min at severe wear, corresponding to a reduction of nearly 2.22%**.** In addition, the flow ripple increases significantly from 0.37% to about 4.88%**,** which indicates that the pump discharge becomes more

unsteady under worn conditions. This happens because the increased piston-cylinder clearance produces higher internal leakage, thereby reducing the useful delivered flow. Hence, Fig. 9 clearly demonstrates that progressive wear causes a noticeable deterioration in the delivery-flow characteristics of the radial piston pump.

Figure 10 shows the effect of progressive piston-cylinder wear on the shaft torque of the nine-piston radial piston pump. In continuation of the leakage, pressure, and flow results presented in Figs. 7–9, an increase in wear has also resulted in a considerable deterioration of the torque characteristics. The mean shaft torque decreases from approximately 179.62 N-m for the healthy pump to 171.80 N-m at 100% wear. More importantly, the torque ripple increases from about 1.95% to 10.95% with increasing piston-cylinder clearance. This behaviour is mainly associated with the non-uniform contribution of the worn piston during the delivery stroke, together with the increased leakage and pressure fluctuation observed in the previous results. Thus, the results clearly demonstrate that severe piston-cylinder wear not only reduces the pressure and flow performance but also produces significant shaft-torque oscillation, which establishes the need for the proposed HHO-Fuzzy-FOPID controller for torque-ripple suppression**.**

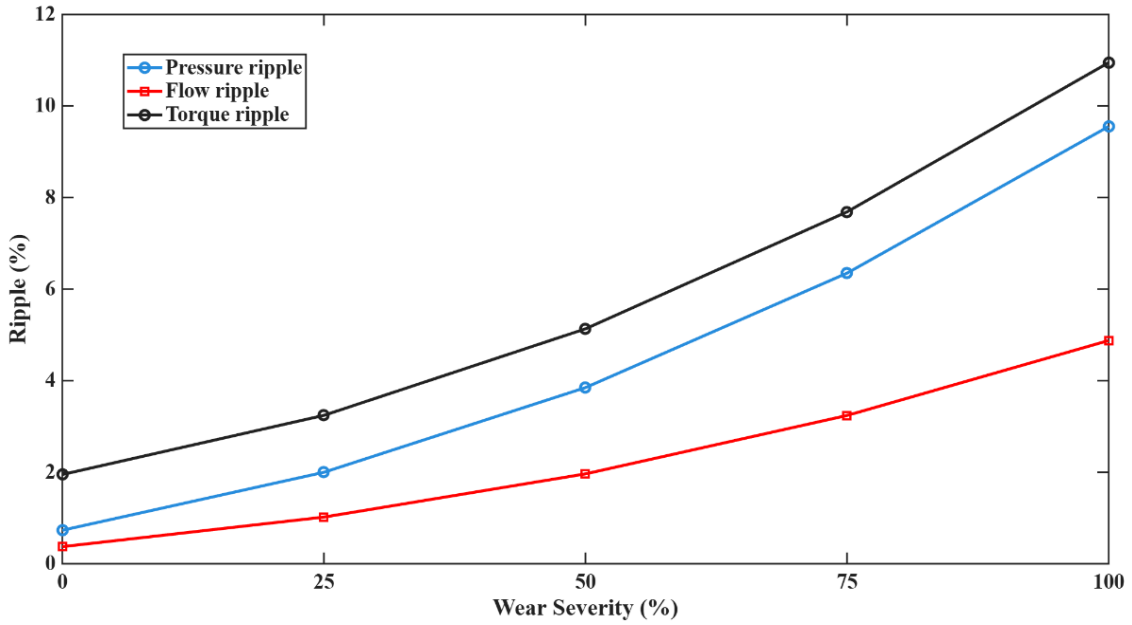


Fig. 11. Variation of pressure ripple, flow ripple, and shaft-torque ripple with piston-cylinder wear severity in the nine-piston radial piston pump.

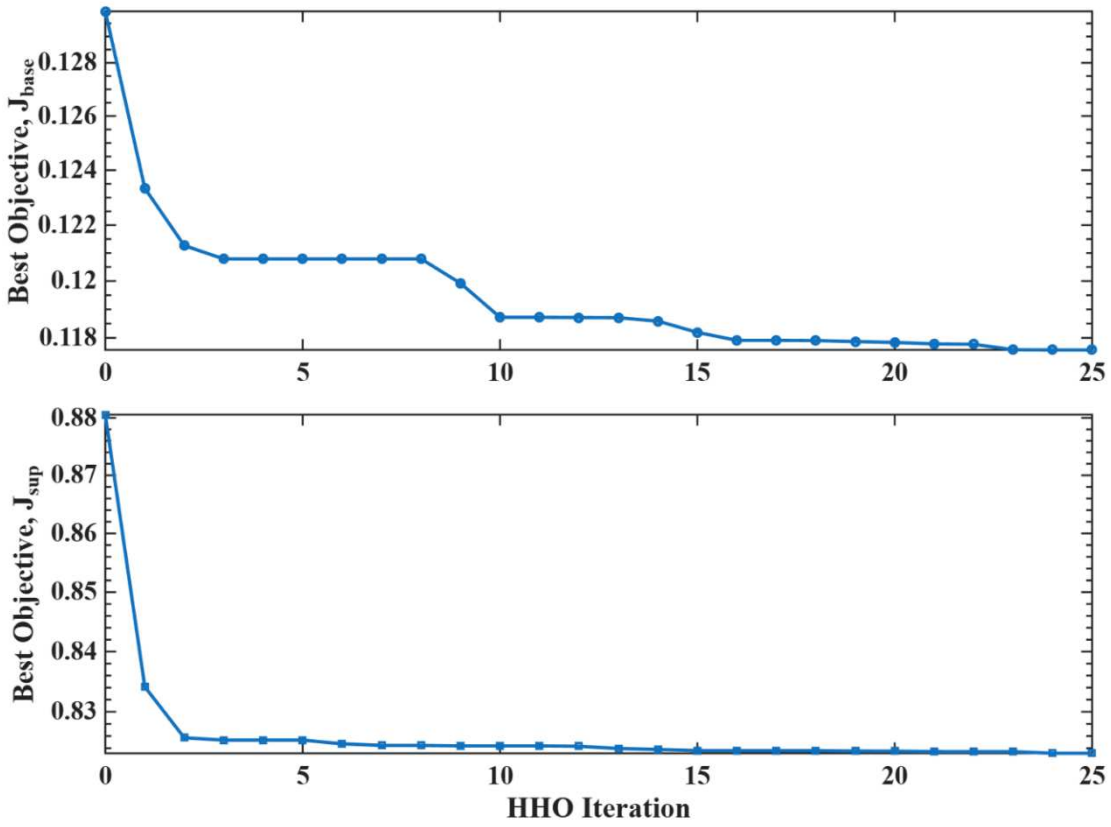


Fig. 12. Convergence characteristics of Harris Hawks Optimization for the proposed HHO-Fuzzy-FOPID controller: (a) optimization of the base FOPID parameters under progressive wear conditions and (b) optimization of the fuzzy supervisory parameters under severe piston-cylinder wear.

Figure 11 shows the variation of pressure ripple, flow ripple, and shaft-torque ripple with increasing piston-cylinder wear. It is observed that all three ripple values increase continuously from healthy condition to severe wear. The pressure ripple increases from 0.73% to 9.55%**,** the flow ripple increases from 0.37% to 4.88%**,** and the torque ripple increases from 1.95% to 10.95%**.** This result clearly confirms that progressive wear makes the pump output increasingly unsteady. This behavior is directly related to the earlier results. The increased piston-cylinder clearance produces higher leakage, which reduces delivery pressure and flow, and finally leads to larger torque oscillations. Therefore, Fig. 11 provides a compact summary of the wear-induced dynamic degradation of the pump and strongly supports the need for the proposed HHO-Fuzzy-FOPID control strategy**.**

Figure 12 presents the convergence behaviour of the Harris Hawks Optimization used for tuning the proposed Fuzzy-FOPID controller. In the first stage, the FOPID parameters have been optimized considering all wear conditions, whereas in the second stage the fuzzy supervisory parameters have been optimized under the severe-wear condition. The progressive reduction of the objective function with iteration indicates that HHO effectively searches the controller-parameter space and approaches a stable optimum solution.

The optimization has considered pressure and flow tracking errors together with pressure, flow, and shaft-torque ripples. In particular, the severe-wear supervisory optimization gives greater importance to torque-ripple reduction. Therefore, the convergence behaviour provides a direct justification for using the HHO-Fuzzy-FOPID controller for simultaneous pressure-flow regulation and torque-ripple suppression in the worn radial piston pump. The optimized parameters of the proposed HHO-Fuzzy-FOPID controller obtained through the two-stage HHO procedure are summarized in Table 4. The base FOPID parameters were optimized in the first stage, followed by optimization of the fuzzy supervisory scaling parameters under the severe-wear condition.

The optimized parameters obtained through the two-stage HHO procedure are summarized in Table 4. In Stage 1, the base FOPID parameters have been optimized considering the combined pressure, flow, ripple, and transient-performance indices, resulting in an objective-function value of 0.1205**.** In Stage 2, the fuzzy supervisory parameters have been optimized under the severe-wear condition, yielding an objective value of 0.7731**.** Since the two stages use different objective-function formulations and normalization factors, these values are not directly comparable; rather, they indicate the convergence of the corresponding optimization stages toward their respective optimum solutions.

The convergence characteristics of both optimization stages are shown in Fig. 12. The continuous reduction and subsequent stabilization of the objective functions indicate the effective convergence of the Harris Hawks Optimization and justify the optimized parameter selection used in the subsequent controller-performance analysis.

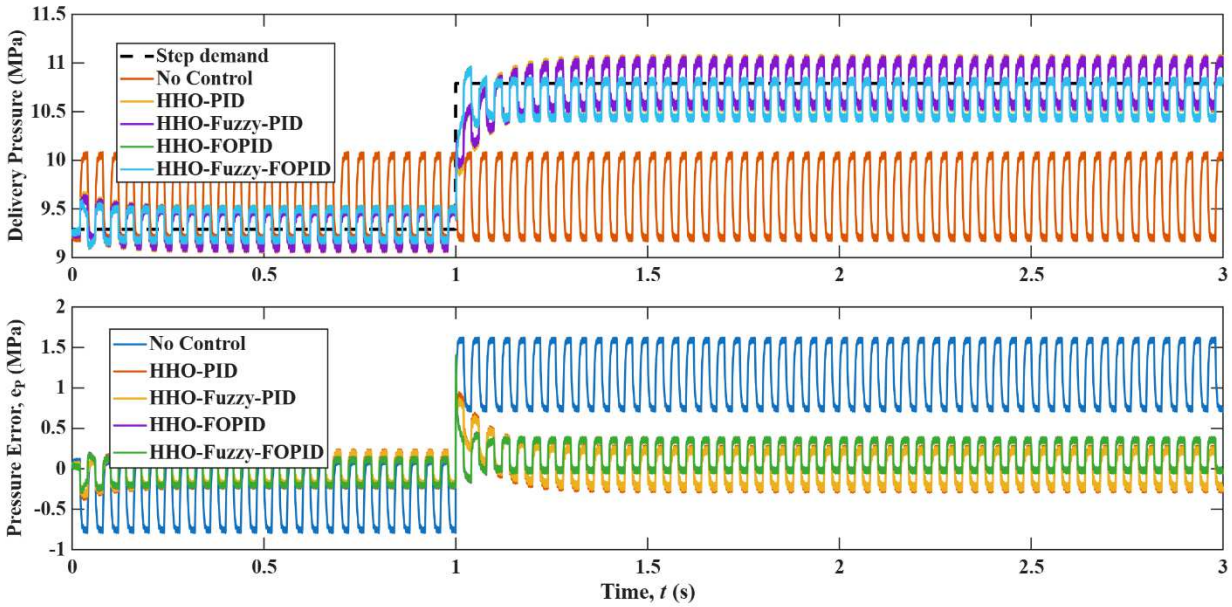


Fig. 13. Step-pressure regulation performance of different HHO-tuned controllers under severe piston-cylinder wear: (a) pressure tracking for a 9.29–10.79 MPa step demand and (b) corresponding pressure tracking error.

Figure 13 presents the step-pressure regulation performance of the different controllers under severe piston-cylinder wear. The pressure demand has been increased from 9.29 MPa to 10.79 MPa at t=1 s**,** while the severe-wear condition has been maintained throughout the simulation. The uncontrolled pump shows a large pressure deviation and is unable to follow the required pressure demand satisfactorily. All HHO-tuned controllers significantly improve the pressure response. Among them, the HHO-Fuzzy-PID gives the lowest pressure RMSE, whereas the proposed HHO-Fuzzy-FOPID provides a faster rise response and the lowest overshoot, indicating improved transient regulation under the worn condition. The fractional-order dynamics together with fuzzy gain adaptation enable the controller to respond rapidly to the demand change while limiting excessive pressure oscillation. Hence, the proposed controller provides a favorable compromise between tracking accuracy, transient response, and pressure smoothness under severe piston-cylinder wear.

Figure 14 presents the delivery-flow response for the same step-demand condition considered in Fig. 13. Severe piston-cylinder wear causes a considerable flow deficit in the uncontrolled case due to increased internal leakage. All HHO-tuned controllers improve the flow response, with the proposed HHO-Fuzzy-FOPID maintaining close tracking of the required flow while providing a smooth transient response. Together with the pressure results, this demonstrates the capability of the proposed controller to achieve effective pressure–flow regulation under worn pump conditions**.**

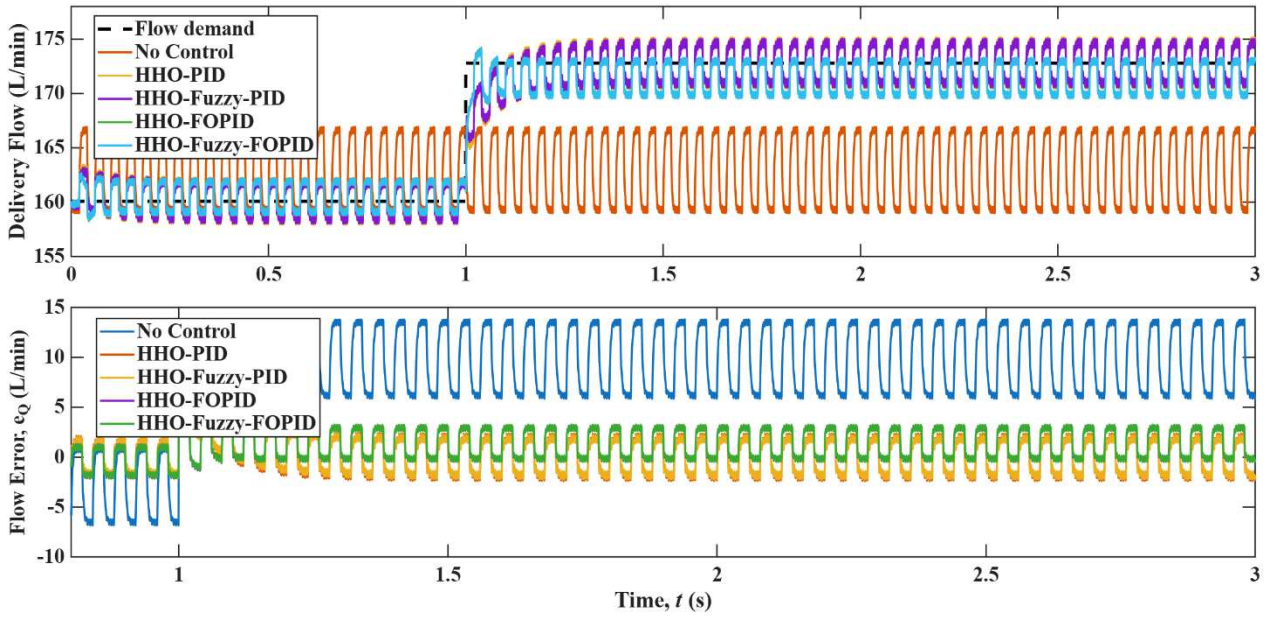


Fig. 14. Step-flow regulation performance of different HHO-tuned controllers under severe piston-cylinder wear: (a) delivery-flow tracking for the 9.29–10.79 MPa step demand and (b) corresponding flow tracking error.

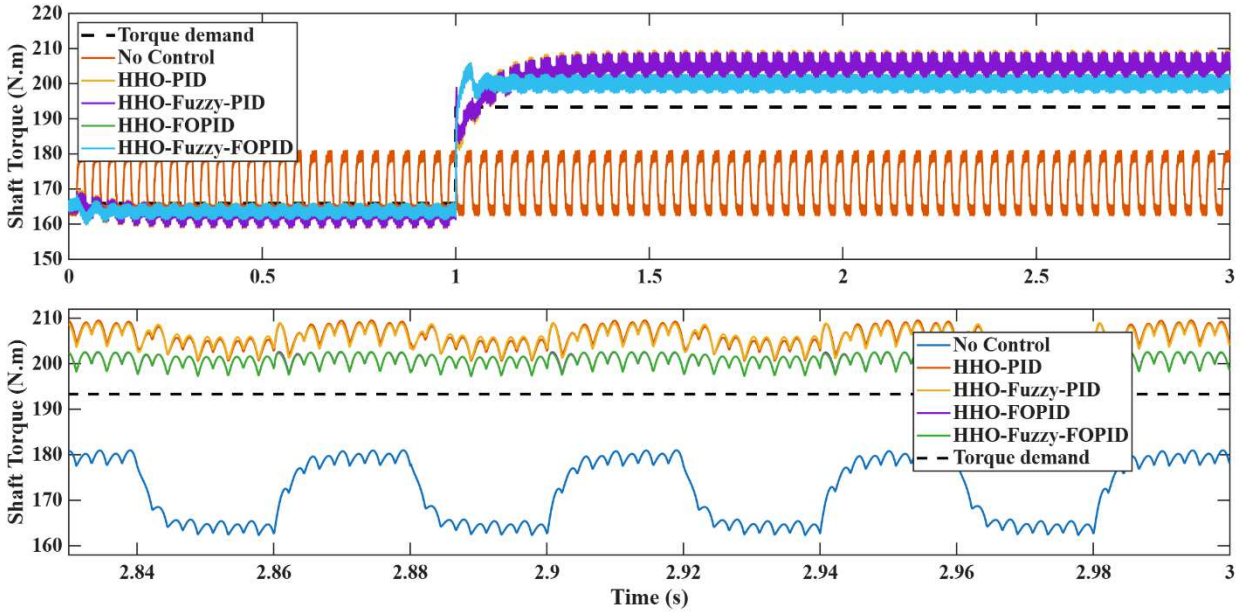


Fig. 15. Shaft-torque regulation under severe piston-cylinder wear for the 9.29–10.79 MPa step demand: (a) torque-tracking response and (b) enlarged steady-state torque-ripple comparison.

Figure 15 presents the shaft-torque response under the same step-demand condition considered in Figs. 13 and 14. Under severe piston-cylinder wear, the uncontrolled pump shows a considerable torque deficit and a high steady-state torque ripple of about 10.83%**.** The application of the HHO-based controllers substantially improves the torque response and suppresses the oscillatory behavior. In particular, the fractional-order controllers provide noticeably better torque regulation than the conventional PID-based schemes. The proposed HHO-Fuzzy-FOPID gives the lowest torque RMSE of approximately 7.57 N·m and the lowest torque MAE of about 7.44 N·m, indicating improved overall torque tracking under severe wear. Its steady-state torque ripple is approximately 2.71%**,** which is very close to the 2.67% obtained with HHO-FOPID. These results show that the proposed controller maintains effective torque regulation while simultaneously supporting the pressure–flow tracking requirements of the worn radial piston pump.

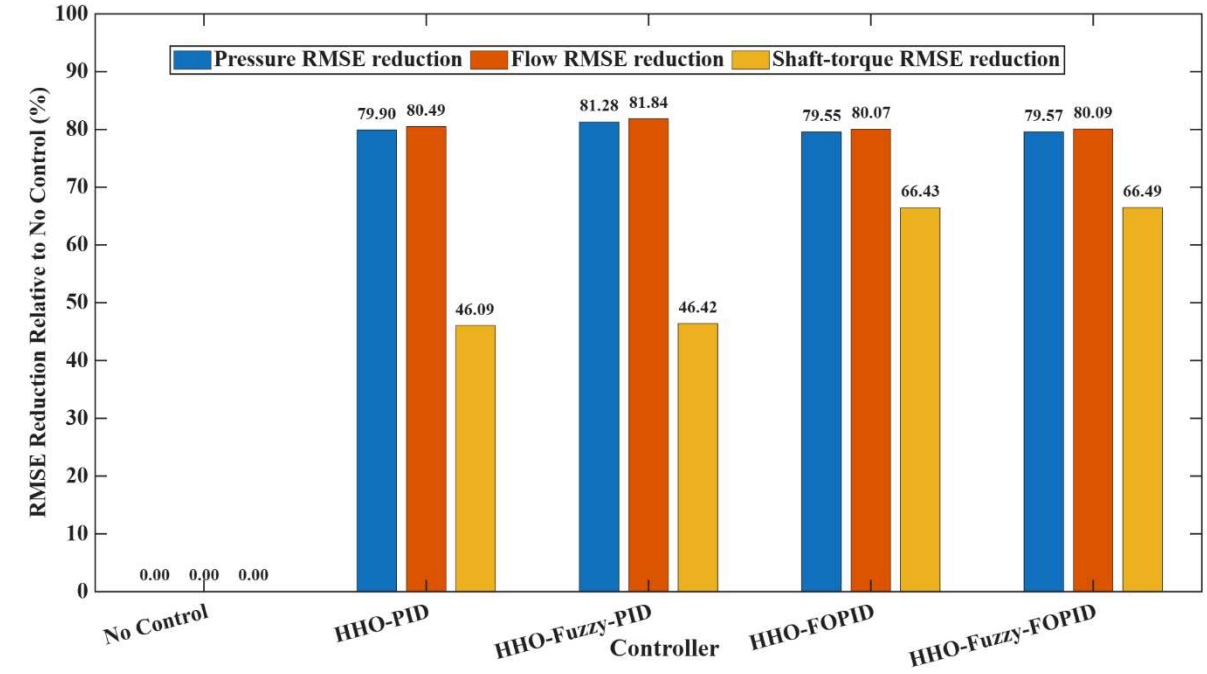


Fig. 16. Percentage reduction in pressure, flow, and shaft-torque RMSE of different HHO-based controllers under severe piston-cylinder wear for the 9.29–10.79 MPa step demand, taking the uncontrolled response as the reference case.

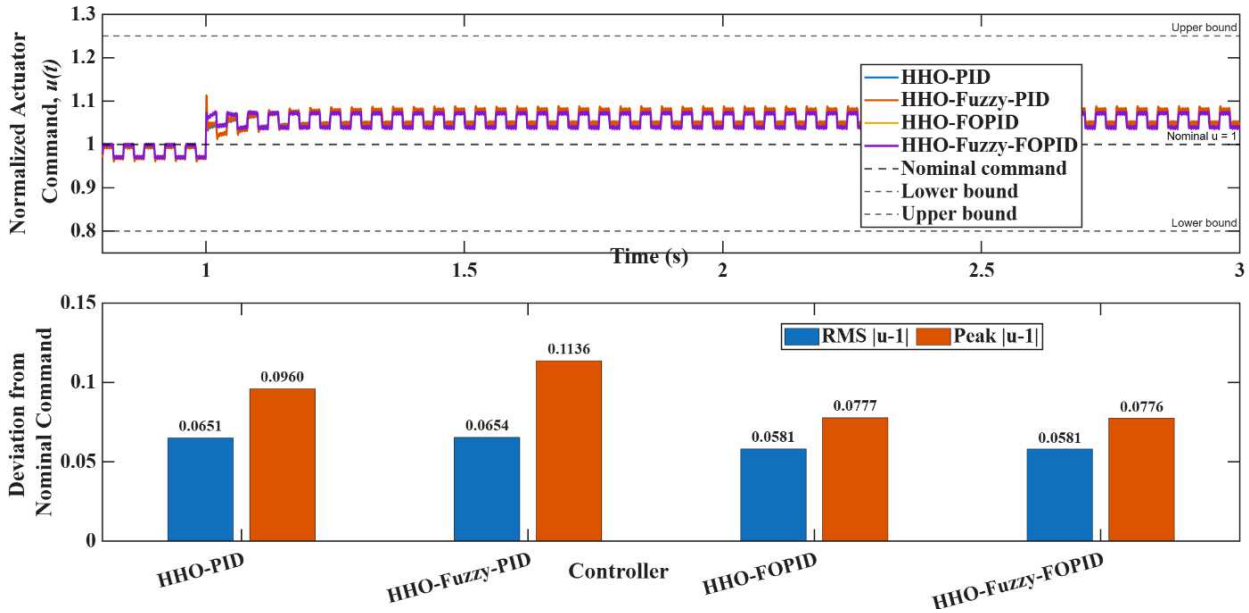


Fig. 17. Control-effort comparison of the HHO-based controllers under severe piston-cylinder wear for the 9.29–10.79 MPa step demand: (a) normalized actuator command and (b) corresponding RMS and peak control deviations from the nominal command.

Figure 16 presents the percentage reduction in pressure, flow, and shaft-torque RMSE under severe piston-cylinder wear, taking the uncontrolled pump response as the reference case. In this representation, a higher percentage indicates better controller performance. It can be observed that all HHO-based controllers significantly improve the pump response compared with the

uncontrolled worn condition. The HHO-Fuzzy-PID controller provides slightly larger pressure and flow error reductions, whereas the proposed HHO-Fuzzy-FOPID gives the highest torque-error reduction among the compared controllers and also the highest overall combined improvement. Specifically, the proposed controller reduces the pressure, flow, and torque RMSE by approximately 79.56%**,** 80.09%**,** and 66.49%**,** respectively. Therefore, the revised comparison clearly indicates that the proposed HHO-Fuzzy-FOPID controller provides the best overall balance between hydraulic tracking and mechanical torque regulation under severe wear, which strongly supports the main objective of the present study.

Figure 17 compares the actuator commands required by the different controllers under the same severe-wear step-demand condition used in Figs. 13–16. All control signals remain within the prescribed actuator limits, indicating bounded controller operation without saturation. The PID-based controllers require comparatively larger control deviations following the pressure-demand change, whereas the fractional-order controllers operate with lower control effort. In particular, the proposed HHO-Fuzzy-FOPID gives an RMS control deviation of approximately 0.0581 and a peak deviation of about 0.0776**,** which are the lowest among the compared controllers. This shows that the improved combined pressure–flow–torque regulation is achieved without excessive actuator action, supporting the practical suitability of the proposed controller for the worn radial piston pump.

Figure 18 shows the robustness of the proposed HHO-Fuzzy-FOPID controller under different piston-cylinder wear severities using the same step-demand condition considered in the previous figures. As the wear level increases from the healthy condition to 100% wear, the pressure, flow, and torque tracking errors increase gradually because the enlarged clearance causes higher internal leakage and greater dynamic disturbance in the pump. However, the increase in error remains well controlled over the full wear range. The pressure RMSE increases from about 0.114 MPa in the healthy case to nearly 0.253 MPa at 100% wear, while the flow RMSE rises from approximately 0.94 L/min to 2.08 L/min**.** Similarly, the torque RMSE increases from about 4.71 N·m to 7.57 N·m**.** Despite this degradation, the final shaft-torque ripple remains below 3% for all wear conditions. These results confirm that the proposed controller maintains stable and effective pressure–flow–torque regulation over a wide range of wear severities, thereby demonstrating strong robustness for practical worn-pump operation.

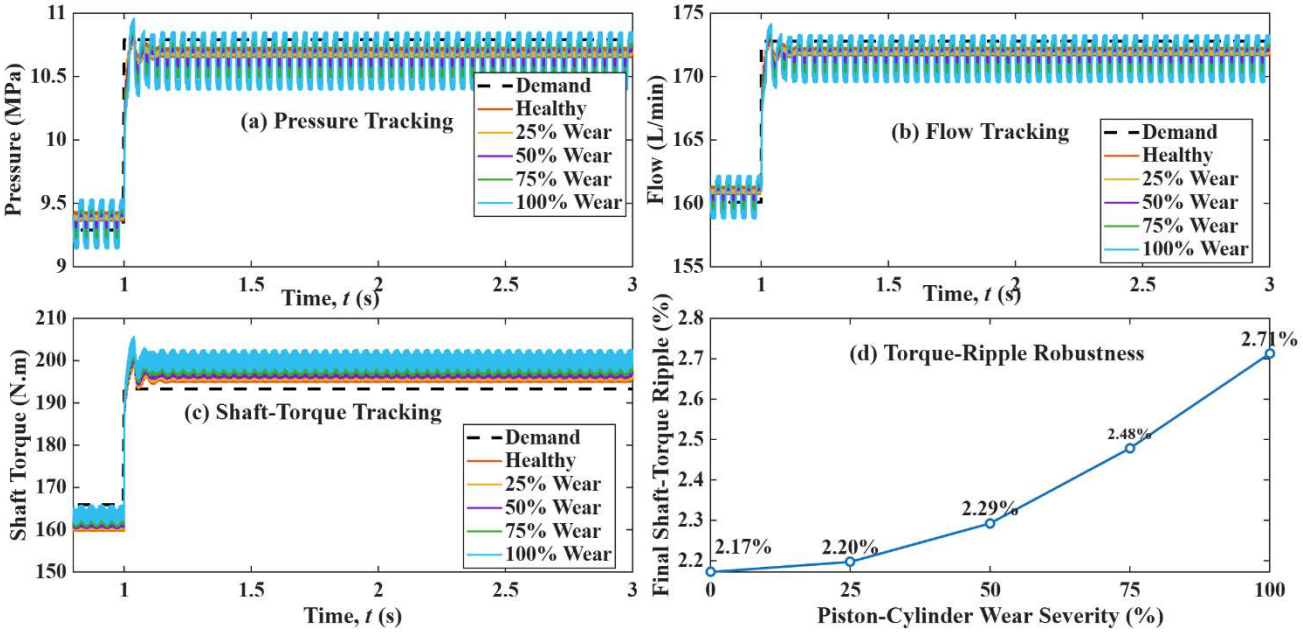


Fig. 18. Robustness of the proposed HHO-Fuzzy-FOPID controller under progressive piston-cylinder wear for the 9.29–10.79 MPa step demand: (a) pressure tracking, (b) flow tracking, (c) shaft-torque tracking, and (d) final torque-ripple variation with wear severity.

6. Conclusions and future work

In the present work, an HHO-tuned Fuzzy-FOPID controller has been developed for the regulation of pressure and flow and for reducing shaft-torque ripple in a worn radial piston pump. The mathematical model has first been validated and then used for a nine-piston pump with progressive piston-cylinder wear. The results have shown that the increase in clearance causes higher internal leakage, which reduces the delivery pressure and flow and increases the shaft-torque fluctuation. Under the severe-wear condition, the proposed controller has shown a better overall balance between hydraulic and mechanical performance. Compared with the uncontrolled pump, the pressure, flow, and torque RMSE have been reduced by about 79.56%, 80.09%, and 66.49%, respectively. The controller has also operated within the specified actuator limits and has maintained stable performance from the healthy condition up to 100% wear. These results indicate that the proposed method is suitable for maintaining pressure-flow performance while limiting torque fluctuation in a worn radial piston pump.

In future work, the proposed controller can be tested experimentally and through hardware-in-the-loop implementation. The study can also be extended to multiple worn pistons, combined faults, variable speed and load conditions, temperature-dependent oil properties, and measurement noise. An online wear-estimation method may also be included so that the controller parameters can be adjusted according to the actual condition of the pump.

Acknowledgements

Dr. Neeraj Kumar gratefully acknowledges the Department of Robotics and Automation, Symbiosis Institute of Technology (SIT), Pune Campus, Symbiosis International (Deemed University), Pune, India, for providing the academic support and research facilities that facilitated the present research.

Funding

This research received no specific grant or financial support from any funding agency.

Data Availability

The data generated and analyzed during the current study are available from the corresponding author on reasonable request.

Competing Interests

The authors declare that they have no known competing financial interests or personal relationships that could have influenced the work reported in this manuscript.

References

[1] M. Radosavljevic, R. Petrovic, B. Zezelj, D. Belovic, S. Cvejic, Mathematical modeling and experimental tests of working parameters of piston-radial pumps in hydraulic systems of mobile machines, Applied Sciences 14 (2024) 9979. https://doi.org/10.3390/app14219979.

[2] M. Zielinski, A. Myszkowski, M. Pelic, R. Staniek, Low-speed radial piston pump as an effective alternative power transmission for small hydropower plants, Renewable Energy 182 (2022) 1012-1027. https://doi.org/10.1016/j.renene.2021.11.014.

[3] L. Kumar, N.P. Mandal, Reduced flow fluctuation of radial piston pump with silencing groove valve plate, International Journal of Fluid Machinery and Systems 15(1) (2022) 38-55. https://doi.org/10.5293/IJFMS.2022.15.1.038.

[4] L. Kumar, N.P. Mandal, Analysis of pressure at transition zone of valve plate of radial piston pump, Engineering Research Express 4 (2022) 035024. https://doi.org/10.1088/2631-8695/ac84c2.

[5] L. Kumar, N.P. Mandal, Effect of silencing groove in valve plate on efficiency of radial piston pump, International Journal of Fluid Machinery and Systems 16(2) (2023) 227-241. https://doi.org/10.5293/IJFMS.2023.16.2.227.

[6] L. Kumar, N.P. Mandal, Pressure control of variable displacement radial piston pump with PID controller, Materials Today: Proceedings 45 (2021) 5158-5165. https://doi.org/10.1016/j.matpr.2021.01.692.

[7] L. Kumar, N.P. Mandal, Pressure control of fixed displacement variable speed radial piston pump using PID controller, Materials Today: Proceedings 56 (2022) 1840-1846. https://doi.org/10.1016/j.matpr.2021.11.034.

[8] J.M. Bergada, S. Kumar, D.Ll. Davies, J. Watton, A complete analysis of axial piston pump leakage and output flow ripples, Applied Mathematical Modelling 36(4) (2012) 1731-1751. https://doi.org/10.1016/j.apm.2011.09.016.

[9] B. Xu, K.-M. Lee, Y. Song, Q. Wang, H. Yang, A numerical and experimental investigation of parametric effect on flow ripple, Proceedings of the Institution of Mechanical Engineers, Part C: Journal of Mechanical Engineering Science 229(16) (2015) 2939-2951. https://doi.org/10.1177/0954406214564585.

[10] J. Ma, B. Xu, H. Yang, Flow ripple of axial piston pump with computational fluid dynamic simulation using compressible hydraulic oil, Chinese Journal of Mechanical Engineering 23(1) (2010) 45-52. https://doi.org/10.3901/CJME.2010.01.045.

[11] S. Ye, J. Zhang, B. Xu, S. Zhu, J. Xiang, H. Tang, Theoretical investigation of the contributions of the excitation forces to the vibration of an axial piston pump, Mechanical Systems and Signal Processing 129 (2019) 201-217. https://doi.org/10.1016/j.ymssp.2019.04.032.

[12] H. Hong, C. Zhao, B. Zhang, D. Bai, H. Yang, Flow ripple reduction of axial-piston pump by structure optimizing of outlet triangular damping groove, Processes 8(12) (2020) 1664. https://doi.org/10.3390/pr8121664.

[13] H. Hong, B. Zhang, M. Yu, Q. Zhong, H. Yang, Analysis and optimization on U-shaped damping groove for flow ripple reduction of fixed displacement axial-piston pump, International Journal of Fluid Machinery and Systems 13(1) (2020) 126-135. https://doi.org/10.5293/IJFMS.2020.13.1.126.

[14] S. Ye, J. Zhang, B. Xu, W. Song, L. Chen, H. Shi, S. Zhu, Experimental and numerical studies on erosion damage in damping holes on the valve plate of an axial piston pump, Journal of Mechanical Science and Technology 31(9) (2017) 4285-4295. https://doi.org/10.1007/s12206-017-0827-4.

[15] N.D. Manring, Y. Zhang, The improved volumetric-efficiency of an axial-piston pump utilizing a trapped-volume design, Journal of Dynamic Systems, Measurement, and Control 123(3) (2001) 479-487. https://doi.org/10.1115/1.1389311.

[16] Y. Pan, Y. Li, D. Liang, The influence of dynamic swash plate vibration on outlet flow ripple in constant power variable-displacement piston pump, Proceedings of the Institution of Mechanical Engineers, Part C: Journal of Mechanical Engineering Science 233(14) (2019) 4914-4933. https://doi.org/10.1177/0954406219840379.

[17] D. Bensaad, A. Soualhi, F. Guillet, A new leaky piston identification method in an axial piston pump based on the extended Kalman filter, Measurement 148 (2019) 106921. https://doi.org/10.1016/j.measurement.2019.106921.

[18] Y. Lin, H. Wang, H. Chen, T. Wang, W. Feng, Q. Bao, L. Ge, H. Hao, Assessment method for wear severity in axial piston pumps based on dynamic identification of leakage coefficient, Proceedings of the Institution of Mechanical Engineers, Part C: Journal of Mechanical Engineering Science (2026), online first. https://doi.org/10.1177/09544062251408133.

[19] Q. Chao, Y. Hu, C. Liu, Physics informed neural networks for detecting the wear of friction pairs in axial piston pumps, Reliability Engineering & System Safety 261 (2025) 111144. https://doi.org/10.1016/j.ress.2025.111144.

[20] C. Dong, J. Tao, H. Sun, Q. Wei, H. Tan, C. Liu, Innovative fault diagnosis for axial piston pumps: A physics-informed neural network framework predicting pump flow ripple, Mechanical Systems and Signal Processing 225 (2025) 112274. https://doi.org/10.1016/j.ymssp.2024.112274.

[21] W. Kemmetmuller, F. Fuchshumer, A. Kugi, Nonlinear pressure control of self-supplied variable displacement axial piston pumps, Control Engineering Practice 18(1) (2010) 84-93. https://doi.org/10.1016/j.conengprac.2009.09.006.

[22] B. Helian, P. Mustalahti, J. Mattila, Z. Chen, B. Yao, Adaptive robust pressure control of variable displacement axial piston pumps with a modified reduced-order dynamic model, Mechatronics 87 (2022) 102879. https://doi.org/10.1016/j.mechatronics.2022.102879.

[23] P. Zhang, Y. Li, Research on control methods for the pressure continuous regulation electrohydraulic proportional axial piston pump of an aircraft hydraulic system, Applied Sciences 9(7) (2019) 1376. https://doi.org/10.3390/app9071376.

[24] G. Wrat, M. Bhola, P. Ranjan, S.K. Mishra, J. Das, Energy saving and Fuzzy-PID position control of electro-hydraulic system by leakage compensation through proportional flow control valve, ISA Transactions 101 (2020) 269-280. https://doi.org/10.1016/j.isatra.2020.01.003.

[25] N. Wang, J. Wang, Z. Li, X. Tang, D. Hou, Fractional-order PID control strategy on hydraulic-loading system of typical electromechanical platform, Sensors 18(9) (2018) 3024. https://doi.org/10.3390/s18093024.

[26] A. Maddahi, N. Sepehri, W. Kinsner, Fractional-order control of hydraulically powered actuators: Controller design and experimental validation, IEEE/ASME Transactions on Mechatronics 24(2) (2019) 796-807. https://doi.org/10.1109/TMECH.2019.2894105.

[27] I. Podlubny, Fractional-order systems and PIλDμ-controllers, IEEE Transactions on Automatic Control 44(1) (1999) 208-214. https://doi.org/10.1109/9.739144.

[28] P. Shah, S. Agashe, Review of fractional PID controller, Mechatronics 38 (2016) 29-41. https://doi.org/10.1016/j.mechatronics.2016.06.005.

[29] M. Al-Dhaifallah, N. Kanagaraj, K.S. Nisar, Fuzzy fractional-order PID controller for fractional model of pneumatic pressure system, Mathematical Problems in Engineering 2018 (2018) 5478781. https://doi.org/10.1155/2018/5478781.

[30] T. Piraisoodi, W.I.M. Siluvairaj, M.A.K. Kappuva, Multi-objective robust fuzzy fractional order proportional-integral-derivative controller design for nonlinear hydraulic turbine governing system using evolutionary computation techniques, Expert Systems 36(2) (2019) e12366. https://doi.org/10.1111/exsy.12366.

[31] A.A. Heidari, S. Mirjalili, H. Faris, I. Aljarah, M. Mafarja, H. Chen, Harris hawks optimization: Algorithm and applications, Future Generation Computer Systems 97 (2019) 849-872. https://doi.org/10.1016/j.future.2019.02.028.

[32] N.H. Mohamad Ali, R. Ghazali, H.I. Jaafar, M.F. Ghani, C.C. Soon, Z. Has, Hybrid fuzzy-fractional order PID control for industrial hydraulic actuators system: Experimental study, International Journal of Robotics and Control Systems 6(1) (2026) 224-242. https://doi.org/10.31763/ijrcs.v6i1.2045.